JCI insight

S-nitrosylation of Connexin43 hemichannels elicits cardiac stress induced arrhythmias in Duchenne Muscular Dystrophy mice

Mauricio A. Lillo, … , Diego Fraidenraich, Jorge E. Contreras

JCI Insight. 2019. https://doi.org/10.1172/jci.insight.130091.

Research In-Press Preview **Muscle biology**

Patients with Duchene Muscular Dystrophy (DMD) commonly present severe ventricular arrhythmias that contribute to heart failure. Arrhythmias and lethality are also consistently observed in adult Dmd^{mdx} mice, a mouse model of DMD, after acute β-adrenergic stimulation. These pathological features were previously linked to aberrant expression and remodeling of the cardiac gap junction protein connexin 43 (Cx43). Here, we report that remodeled Cx43 protein forms Cx43 hemichannels in the lateral membrane of Dmd^{mdx} cardiomyocytes and that the β -adrenergic agonist isoproterenol (Iso) aberrantly activates these hemichannels. Block of Cx43 hemichannels or a reduction in Cx43 levels (using Dmd^{mdx}:$Cx43^{+/-}$ mice) prevents the abnormal increase in membrane permeability, plasma membrane depolarization and Iso-evoked electrical activity in these cells. Additionally, Iso treatment promotes nitric oxide (NO) production and S-nitrosylation of Cx43 hemichannels in Dmd^{mdx} heart. Importantly, inhibition of NO production prevents arrhythmias evoked by Iso. We found that NO directly activates Cx43 hemichannels by S-nitrosylation of cysteine at the position 271. Our results demonstrate that opening of remodeled and S-nitrosylated Cx43 hemichannels play a key role in the development of arrhythmias in DMD mice and may serve as therapeutic targets to prevent fatal arrhythmias in DMD patients.

S-nitrosylation of Connexin43 hemichannels elicits cardiac stress-induced arrhythmias in Duchenne Muscular Dystrophy mice.

Mauricio A. Lillo[1], Eric Himelman[2], Natalia Shirokova[1], Lai-Hua Xie[2], Diego Fraidenraich[2], Jorge E. Contreras[1‡]

Affiliations:

1 Department of Pharmacology, Physiology and Neuroscience, Rutgers University, New Jersey Medical School

2 Department of Cell Biology and Molecular Medicine. Rutgers University, New Jersey Medical School

Corresponding Author:

[‡]Jorge E. Contreras; Medical Sciences Building I-615; 185 S. Orange Avenue, Newark, NJ 07103.
contrejo@njms.rutgers.edu

Keywords: Connexin, hemichannels, arrhythmia

Abstract

Patients with Duchene Muscular Dystrophy (DMD) commonly present severe ventricular arrhythmias that contribute to heart failure. Arrhythmias and lethality are also consistently observed in adult *Dmd*^{mdx} mice, a mouse model of DMD, after acute β-adrenergic stimulation. These pathological features were previously linked to aberrant expression and remodeling of the cardiac gap junction protein connexin 43 (Cx43). Here, we report that remodeled Cx43 protein forms Cx43 hemichannels in the lateral membrane of *Dmd*^{mdx} cardiomyocytes and that the β -adrenergic agonist isoproterenol (Iso) aberrantly activates these hemichannels. Block of Cx43 hemichannels or a reduction in Cx43 levels (using *Dmd*^{mdx}:Cx43$^{+/-}$ mice) prevents the abnormal increase in membrane permeability, plasma membrane depolarization and Iso-evoked electrical activity in these cells. Additionally, Iso treatment promotes nitric oxide (NO) production and S-nitrosylation of Cx43 hemichannels in *Dmd*^{mdx} heart. Importantly, inhibition of NO production prevents arrhythmias evoked by Iso. We found that NO directly activates Cx43 hemichannels by S-nitrosylation of cysteine at the position 271. Our results demonstrate that opening of remodeled and S-nitrosylated Cx43 hemichannels play a key role in the development of arrhythmias in DMD mice and may serve as therapeutic targets to prevent fatal arrhythmias in DMD patients.

Introduction

Duchene Muscular Dystrophy (DMD) is an incurable, progressive muscle disease that affects approximately one in 3,500 male births (1). DMD is caused by lack of the functional structural protein dystrophin. Absence of dystrophin increases cellular fragility resulting in recurrent skeletal and cardiac muscle damage during contraction (2). Currently, steroid therapy and assisted ventilation help to combat skeletal muscle related respiratory dysfunction and significantly prolong the lives of DMD patients. However, cardiac dysfunction (e.g. reduced contractility and arrhythmias) is becoming a prominent contributor to DMD pathology (3, 4) and over 40% of patients die from heart failure (1, 5).

Current treatments to attenuate DMD cardiomyopathies rely mainly on angiotensin-converting enzyme (ACE) inhibitors, β-adrenergic blockers and avoidance of high-intensity adrenaline inducing activities (6, 7). Indeed, β-adrenergic signaling is highly dysregulated in DMD hearts. For example, cardiac stress induces oxidative stress and hyperactivity of Ca^{2+}/calmodulin-dependent protein kinase II (CaMKII) and ryanodine receptor 2 (RyR2), which triggers ventricular arrhythmias in young *Dmd*^{mdx} mice (8, 9). At later stages of the disease "leaky" RyR2 channels contribute to aberrant Ca^{2+} release from the sarcoplasmic reticulum. This Ca^{2+} leak triggers a signaling pathway that promotes plasma membrane potential (*Vm*) depolarization and, consequently, delayed after depolarizations (DAD) (10). However, plasma membrane channels/transporters responsible for changes in *Vm* in *Dmd*^{mdx} cardiomyocytes remains elusive.

In the heart, cardiomyocytes are arranged laterally end to end and connected through intercalated discs. The intercalated discs of healthy cardiomyocytes contain gap junctions, which act as low resistance channels to an opposing cardiomyocyte (11). Connexin 43 (Cx43) is the most

abundant connexin isoform and is found in the working myocardium of the atrium and ventricle as well as in the more distal regions of the Purkinje network (12). The biogenesis of a Cx43 gap junction channel begins with the intracellular assembly of six connexins (Cx) proteins to form a hemichannel, which is then inserted into the plasma membrane. The hemichannel moves to sites of apposition between cells and docks with a hemichannel of an adjacent cell to form a gap junction channel. Importantly, myocytes from diseased hearts display abnormal levels of Cx43 and redistribute to the plasma membrane away from the intercalated discs. This increase of Cx43 in lateralized regions of diseased cardiomyocytes is a phenomenon known as remodeling (13-15). Cx43 remodeling is observed in several pathological cardiac conditions, including ischemia, hypertrophy, heart failure as well as in DMD (13-17).

We have recently proposed that in the heart, remodeled Cx43 proteins at the plasma membrane in *Dmd*^{mdx} mice do not form gap junctions, but instead, undocked hemichannels (16, 18). Thus we hypothesize that β-adrenergic stimulation enhances the activity of remodeled Cx43 hemichannels in *Dmd*^{mdx} hearts, affecting cardiomyocyte membrane excitability and promoting arrhythmias. Here, we tested this idea and demonstrated that β-adrenergic stimulation leads to the opening of Cx43 hemichannels via nitric oxide (NO) production and direct S-nitrosylation of Cx43 proteins. Inhibition of NO synthesis prevented S-nitrosylation of Cx43 and arrhythmias evoked by β-adrenergic stimulation in *Dmd*^{mdx} mice. Consistent with this observation, S-nitrosylation of Cx43 hemichannels resulted in membrane plasma depolarization of *Dmd*^{mdx} cardiomyocytes and subsequent generation of action potentials. Finally, we determined that Cx43 hemichannel activity increases after S-nitrosylation of cysteine 271 in the C-terminal domain. We propose that enhanced S-nitrosylation and opening of remodeled Cx43 hemichannels is critical for the development of arrhythmias in DMD.

Results

Isoproterenol-evoked electrical activity in *Dmd*^{mdx} cardiomyocytes is mediated by Cx43 hemichannels.

We tested the hypothesis that lateralized Cx43 protein forms hemichannels with aberrant activity, which results in increased membrane excitability and favors Iso-induced arrhythmias in *Dmd*^{mdx} cardiomyocytes. Fig. 1A shows representative traces of cardiac action potentials (APs) from WT and *Dmd*^{mdx} isolated cardiomyocytes evoked by an injection of 2 nA current under current-clamp conditions. Treatment of cells with 1µM Iso induced triggered activity (TA) in *Dmd*^{mdx}, but not WT cardiomyocytes. The average number of Iso-induced TA was 63 ± 1.8 and 2 ± 0.5 per minute in *Dmd*^{mdx} and WT cardiomyocytes, respectively (Fig. 1B).

To assess the role of Cx43 hemichannels in Iso-evoked TA, we examined whether the latter is prevented by two different specific Cx43 hemichannel blockers added into the patch pipette; Gap19 peptide (20, 21) (232ng/ µL) or AbCx43 antibody (2.5 ng/ µL) that recognizes the C-terminal domain of Cx43. Iso-evoked TAs were significantly reduced (by ~ 80 %) in *Dmd*^{mdx} cardiomyocytes treated with both Gap19 peptide (8.2 ± 0.6 per minute) or AbCx43 (7.4 ± 0.4 per minute) (Fig. 1A and B). Importantly, blockade of Cx45 hemichannels, a distinct Cx isoform also expressed in cardiomyocytes (12), with an antibody against the Cx45 CT domain, did not prevent the generation of TA (Fig. 1A and B).

Previously, we showed that dystrophic mice with lower levels of Cx43 (*Dmd*^{mdx}*:*Cx43$^{+/-}$) were resistant to Iso-induced arrhythmias (18). *Dmd*^{mdx}*:*Cx43$^{+/-}$ cardiomyocytes display less lateralize Cx43 protein and likely reduced hemichannels activity (18). We asked, therefore, whether dystrophic cardiomyocytes from *Dmd*^{mdx}*:*Cx43$^{+/-}$ mice were less susceptible to Iso-induced TAs. Upon treatment with 1µM Iso, isolated cardiac cells from *Dmd*^{mdx}*:*Cx43$^{+/-}$ displayed a significant

reduction (by ~ 70 %) of TAs compare to *Dmd*^{mdx} cardiomyocytes. Addition of the AbCx43 antibody in the pipette completely prevented the TAs in *Dmd*^{mdx}*:*Cx43$^{+/-}$ cardiomyocytes (Figure 1A). The average number of TA was 18, 4 ± 3.2 and 3.2± 0.8 per minute in *Dmd*^{mdx}*:*Cx43$^{+/-}$ in the absence and presence of AbCx43, respectively (Figure 1B). These data strongly suggest that Iso-evoked TAs in *Dmd*^{mdx} cardiomyocytes are mediated by activity of Cx43 hemichannels.

We next examined whether Iso-induced TAs in *Dmd*^{mdx} cardiomyocytes are associated with changes in the resting membrane potential (*Vm*), which in turn are caused by the altered activity of Cx43 hemichannels. Fig. 1C shows that *Dmd*^{mdx} cardiomyocytes are more depolarized with respect to WT cardiomyocytes under normal conditions, with *Vm* values of -65.3 ± 2.1 mV and -67.8 ± 3.2 mV, respectively. Iso stimulation further depolarized both *Dmd*^{mdx} and WT cardiomyocytes to *Vm* values of -61.4 ± 1.3 mV and -64.6 ± 3.2 mV, respectively. Strikingly, when Gap19 or AbCx43 were added in the pipette solution, *Vm* in *Dmd*^{mdx} cardiomyocytes was returned to values similar to those observed in WT cardiomyocytes. Consistently, *Dmd*^{mdx}*:*Cx43$^{+/-}$ cardiomyocytes in the absence or presence of Iso display resting membrane potential depolarization with *Vm* values of -67.5± 0.9 mV and -65.9 ± 2.4 mV, respectively. These resting membrane potentials values resemble more to those observed in WT cardiomyocytes than *Dmd*^{mdx} cardiomyocytes. Intracellular application of AbCx43 in *Dmd*^{mdx}*:*Cx43$^{+/-}$ cardiomyocytes further prevent isoproterenol-induced resting membrane potential depolarization to *Vm* values of -68.2± 4.9 mV. These data support that plasma membrane depolarization in *Dmd*^{mdx} cardiomyocytes is caused by the altered activity of Cx43 hemichannels.

To demonstrate that Iso-induced depolarization of resting membrane potential plays a crucial role in generating TA in *Dmd*^{mdx} cardiomyocytes, we injected hyperpolarizing currents to maintain the resting membrane potential near –68 mV (the values observed in WT cells before Iso

treatment). Under these conditions, *Dmd*^{mdx} cardiomyocytes treated with Iso displayed a significant reduction of TA events (10.5±0.2 per min) (Figure. S1). Furthermore, *Dmd*^{mdx} cardiomyocytes not treated with Iso, but injected with depolarizing currents to maintain the resting membrane potential near – 61 mV (the value observed after Iso treatment) displayed significant number of TAs (60.3 ± 0.2 per min).

Sodium-calcium exchanger (NCX) activity has been also proposed to promote membrane depolarization and DADs, in cardiac pathologies such as hypoxia-reoxygenation, transverse aortic contraction (TAC) and heart failure (22-25). However, blockade of NCX transporters using the specific inhibitor SEA0400 (26), did not restore Iso-induced resting membrane potential depolarization and TAs (Figure S2) in *Dmd*^{mdx} cardiomyocytes. Taken together our data suggest that Iso treatment produces *Vm* depolarization and consequently, generate TA events in *Dmd*^{mdx} cardiomyocytes mainly via Cx43 hemichannel activity.

To confirm that Iso treatment increases activity of Cx43 hemichannels in the *Dmd*^{mdx} hearts, we developed a semi-quantitative *in-situ* assay utilizing perfused isolated hearts (see methods). Uptake of hemichannel-permeable, plasma membrane-impermeable molecules, such as fluorescent ethidium bromide (EtBr) from the extracellular space is largely used to measure open Cx43 hemichannels (27-29). Under normal conditions, *Dmd*^{mdx} hearts showed about four-fold greater ethidium uptake than WT hearts (Fig. 1D). Iso stimulation significantly increased ethidium uptake in both genotypes, but a significantly larger uptake was detected in *Dmd*^{mdx} hearts (Fig. 1D). *In vivo* treatment with Gap19 via retro-orbital injection prior to Iso administration drastically reduced dye uptake in *Dmd*^{mdx} hearts under both normal and Iso stimulated conditions (Fig. 1D). Moreover, isolated heart from *Dmd*^{mdx}*:*Cx43$^{+/-}$ mice did not display significant ethidium uptake upon isoproterenol treatment (Fig. 1D). The uptake of a Cx43 hemichannel impermeable dye,

propidium iodide (PI), was negligible under basal or Iso-induced conditions, ruling out unspecific dye permeability mediated by plasma membrane breakdown (Fig. S3). These results indicate that the substantial ethidium uptake observed in *Dmd*^{mdx} hearts stimulated with Iso is mediated by the opening of Cx43 hemichannels.

In the next group of experiments, we estimated the amount of lateralized Cx43 hemichannels at the plasma membrane of cardiomyocytes in the intact heart of WT and *Dmd*^{mdx} mice using a modified method of cell-surface protein biotinylation. Immunofluorescence against biotin perfused into whole hearts showed that biotin only reaches the lateral sides of cardiomyocytes, but not the intercalated discs (Fig.2A). Western blot analysis of the biotinylated fraction showed that *Dmd*^{mdx} hearts have significantly higher levels of Cx43 protein at the lateralized region when compared to WT hearts. Iso-treatment increased the levels of lateralized Cx43 in both WT and *Dmd*^{mdx} heart. N-cadherin and endothelial nitric oxide synthase (eNOS) were not detected in the biotinylated fraction, confirming that biotin did not interact with intercalated discs (N-Cadherin) and intracellular (eNOS) proteins (Fig. 2B). Furthermore, biotinylated fraction in *Dmd*^{mdx}*:*Cx43$^{+/-}$ hearts displayed lower levels of Cx43 protein at the lateralized region when compared to *Dmd*^{mdx} hearts (Fig S4). Notably, the amount of lateralized Cx43 hemichannels at the plasma membrane strongly correlates with the levels of ethidium uptake in WT and *Dmd*^{mdx} heart under control conditions and after Iso treatment (Fig. 1D). Overall, our results strongly suggest an important role for Cx43 hemichannels in the pathophysiology of *Dmd*^{mdx} hearts.

Isoproterenol promotes S-nitrosylation and opening of lateralized Cx43 hemichannels in the *Dmd*^{mdx} heart.

β-adrenergic stimulation activates NO synthases (NOS) and promotes S-nitrosylation of several Ca^{2+}-handling proteins in the heart (30, 31). Because opening of Cx43 hemichannels has been linked to NO production in astrocytes (32), we evaluated whether Cx43 is S-nitrosylated in the hearts of WT and *Dmd*^{mdx} mice upon Iso stimulation. Using the biotin switch assay, we found that levels of S-nitrosylated Cx43 in *Dmd*^{mdx} cardiac tissue is almost four-folds greater than in the WT heart under control conditions (Fig. 3A). Iso stimulation resulted in a nearly 2-fold increase in levels of S-nitrosylated Cx43 in both WT and *Dmd*^{mdx} with respect to control (Fig. 3A). S-nitrosylated Cx43 levels in *Dmd*^{mdx}*:*Cx43$^{+/-}$ were also reduced when compared to *Dmd*^{mdx} hearts (Figure S5A). To confirm that S-nitrosylation of Cx43 depends on Iso-induced NO production, both WT and *Dmd*^{mdx} animals were administered 2 mM N^{ω}-nitro-L-arginine (L-NAME) , a non-selective NOS inhibitor (33), in their drinking water for one week prior to Iso stimulation. Following L-NAME treatment, levels of S-nitrosylated Cx43 in both WT and *Dmd*^{mdx} hearts treated with Iso were restored to control levels (Fig. 3A).

To examine the subcellular localization of S-nitrosylated Cx43, we performed the Proximity Ligation Assay (PLA) using antibodies that recognize S-nitrosylated proteins (S-NO) and the C-terminus of Cx43. In WT hearts, S-nitrosylated Cx43 was confined to intercalated discs, and its fluorescence was intensified after mice were injected with Iso (5 mg/kg). In *Dmd*^{mdx} hearts under control conditions, the staining for S-nitrosylated Cx43 was also localized to intercalated discs and was visibly stronger than WT. After treatment with Iso, S-nitrosylated Cx43 found mostly at lateral sides in *Dmd*^{mdx} hearts. Importantly, the S-nitrosylated Cx43 signals were visibly diminished in Iso treated WT and *Dmd*^{mdx} hearts after one week of L-NAME administration in the

drinking water (Fig. 3B). *Dmd*^{mdx}*:*Cx43$^{+/-}$ cardiomyocytes also displayed a significant reduction of S-nitrosylated Cx43 signals compared to *Dmd*^{mdx} and WT hearts in the absence or presence of upon β-adrenergic stress (Fig.S5B). These data confirm that S-nitrosylated Cx43 is localized to the lateral side of *Dmd*^{mdx} cardiomyocytes upon Iso treatment.

To evaluate whether Iso-induced NO production and S-nitrosylation of Cx43 is linked to an increase in Cx43 hemichannel activity, we examined whether Cx43 hemichannel mediated ethidium uptake in perfused WT and *Dmd*^{mdx} hearts is inhibited by the pre-treatment of L-NAME. Ethidium fluorescence increased by about 2-fold with respect to vehicle conditions in the *Dmd*^{mdx} heart after Iso treatment (Fig. 3C). Moreover, L-NAME treatment completely eliminated Iso induced ethidium uptake. These data suggest that β-adrenergic stimulation-induced ethidium uptake in *Dmd*^{mdx} mice results from the opening of S-nitrosylated Cx43 hemichannels.

We also performed biotin switch assay and PLA analysis on heart samples obtained from multiple non-DMD and DMD patients in order to test S-nitrosylation status of Cx43 in humans. Total S-nitrosylated levels of Cx43 in the human DMD hearts were 3-folds higher than that observed in controls (Fig. 3D). PLA analysis confirmed that S-nitrosylated Cx43 is located at the lateral sides of human DMD hearts. Conversely, in non-DMD hearts, S-nitrosylated Cx43 was mainly located at the intercalated discs (Fig. 3E). These findings indicate that S-nitrosylated Cx43 might play an essential role in human DMD cardiomyopathy.

Inhibition of NOS prevents isoproterenol-induced TA and arrhythmias in *Dmd*^{mdx} mice.

Because Iso-evoked opening of Cx43 hemichannels is drastically reduced by inhibiting NO production in *Dmd*^{mdx} hearts (Fig. 3C), we next studied whether TA mediated by Cx43 hemichannels are also affected by inhibition of NO production in Iso-treated *Dmd*^{mdx}

cardiomyocytes. Fig. 4A shows representative action potentials in WT and *Dmd*^{mdx} isolated cardiomyocytes that were evoked by electrical stimulation in control conditions or in the presence of 100 μM L-NAME. Treatment with L-NAME reduced the incidence of Iso-evoked TAs in *Dmd*^{mdx} cardiomyocytes (Fig. 4A and B). Moreover, L-NAME significantly reduced the Iso-induced increase in the resting membrane potential of *Dmd*^{mdx} cardiomyocytes, restoring it to similar values observed in WT cardiomyocytes (Fig. 4C). L-NAME effect on TAs is similar to that observed after the block of Cx43 hemichannels (Fig. 1A and C), supporting the idea that Cx43 hemichannel mediated aberrant electrical activity in *Dmd*^{mdx} cardiomyocytes is likely result of S-nitrosylation of hemichannels.

Since we have proposed that Cx43 hemichannels mediate Iso-induced arrhythmogenesis in *Dmd*^{mdx} mice (16, 18), we next tested whether blockade of NO production reduces arrhythmias. To test this, we performed in vivo electrocardiograms (ECG) in WT and *Dmd*^{mdx} mice under control condition and after L-NAME treatment. Representative ECGs recorded from WT and a *Dmd*^{mdx} mice treated with L-NAME are shown in Fig. 4D. Remarkably, *Dmd*^{mdx} mice treated with L-NAME were protected from Iso-induced arrhythmias (Fig. 4D), evident by a significantly lower arrhythmia score compared to vehicle treated counterparts (Fig. 4E).

Exogenous application of NO induces TA in *Dmd*^{mdx} cardiomyocytes.

To demonstrate a direct role of NO on the generation of TA in *Dmd*^{mdx} cardiomyocytes, we next investigated whether application of a NO donor, sodium 2-(N, N-diethylamino)-diazenolate-2-oxide (DEENO, 1μM), mimics Iso-induced TA. TAs were observed in DEENO treated *Dmd*^{mdx} isolated cardiomyocytes (58.1 ± 4.3 per minute), but not WT (Fig. 5A and B). This value is

comparable to that observed for Iso-induced TA (Fig. 1C). Furthermore, Cx43 hemichannel blockers, Gap19 and AbCx43, largely reduced observed TAs to values of 8.2 ± 0.9 and 7.3 ± 0.8, respectively (Fig. 5A and B). As expected, isolated cardiac cells from *Dmd*^{mdx}*:*Cx43$^{+/-}$ mice display a significant reduction of TAs (10.4 ± 1.2 per minute) upon DEENO stimulation when compare to *Dmd*^{mdx} cardiomyocytes (Fig. 5A and B). In addition, exogenous NO application depolarized the membrane in both WT and *Dmd*^{mdx} cardiomyocytes to *Vm* of -65.9 and -61.8 mV, respectively (Fig. 5C). Cx43 hemichannel blockers and genetic reduction on the levels of Cx43 (*Dmd*^{mdx}*:*Cx43$^{+/-}$) restored the resting membrane potential to those observed in vehicle values (Fig. 5C). Importantly, NO treated *Dmd*^{mdx} cardiomyocytes displayed resting membrane potential values similar to those found in Iso treated cells, thus indicating a similar mechanism of changes in membrane excitability (Fig. 1C). Thus, our findings strongly suggest that Iso, NO and Cx43 hemichannel opening operate in the same signaling pathway that induces TA and arrhythmias in stressed *Dmd*^{mdx} heart.

NO activates Cx43 hemichannels via S-nitrosylation of cysteine 271.

To confirm that NO activates Cx43 hemichannels via S-nitrosylation, we assessed Cx43 hemichannel ionic currents in *Xenopus* oocytes using the two-electrode voltage-clamp technique. Consistent with previous studies, we did not observe noticeable Cx43 hemichannels currents in response to changes in voltage or low extracellular [Ca^{2+}] (27, 34-37). However, treatment of Cx43 expressing oocytes with 10µM DEENO evoked an increase in plasma membrane conductance at all voltages when compared with non-injected oocytes (Fig. 6A). The increase in current induced by NO was blocked when using either Gap19 or AbCx43 (Fig. 6B), confirming that observed current originated from Cx43 hemichannels.

We also found NO induced depolarization of the *Vm* in oocytes expressing Cx43, but not in the non-injected oocytes. Consistently, Gap19 and AbCx43 prevented NO-induced *Vm* depolarization in Cx43 expressing oocytes (Fig. 6C). Extracellular calcium drastically reduces Cx43 open hemichannel probability (27). Consistent with this, NO-induced *Vm* changes in Cx43 expressing oocytes were dependent on extracellular calcium concentrations (Fig. 6D).

The C-terminus of Cx43 is a target for various posttranslational modifications. It includes various phosphorylation sites that affect gap junction plaque formation and stability (38-40). It also contains three cysteines (C260, C271, and C298) that could be targets of S-nitrosylation. Thereby, we deleted C-terminus of Cx43 (CT, Cx43ΔCT) and examined ionic currents in response to DEENO application. Cx43ΔCT expressing oocytes did not display NO-induced hemichannel currents upon stimulation with DEENO (Fig. 7A). We also made single substitutions of cysteines C260S, C271S, C298S of Cx43 with non-polar amino acid serine and tested for NO-induced hemichannel activation. Whereas C260S and C298S mutant hemichannels remained sensitive to NO, C271S mutant completely lost its NO dependence (Fig. 7A). Moreover, DEENO treatment depolarized the resting membrane potential in oocytes expressing C260S and C298S, but not C271S (Fig. 7B).

Although the above data suggests that C271 is critical for NO-induced Cx43 hemichannels opening, we cannot rule out yet the possibility that the deletion of the CT in Cx43 and the C271S mutation *per se* precludes hemichannel opening by affecting gating, independently of lack of nitrosylation at C271. To address this, we tested the NO responses in heteromeric Cx43 and Cx26S17F hemichannels, which are activated by changes in membrane potential (34). Fig. S6A shows representative currents from heteromeric hemichannels formed by combination of Cx43, Cx43ΔCT or Cx43C271S and Cx26S17F (black traces) elicited by depolarizing pulse from -80

mV to 0 mV. In the presence of 10 μM DEENO, heteromeric channels containing the full length Cx43, but not Cx43C271S and Cx43ΔCT, displayed an increase in currents (red traces). Cx26 or Cx26S17F homomeric hemichannels were not sensitive to NO donors (Fig. S6B). Thus, we conclude that the CT of Cx43 mediates NO-induced hemichannel currents via NO modifications at the residue C271.

To biochemically confirm that residue C271 is S-nitrosylated by NO in Cx43 hemichannels, we conducted a biotin switch assay. S-nitrosylated Cx43 was detected in oocytes expressing Cx43, Cx43C260S, and Cx43C298S after the treatment with 10 μM DEENO. Consistent with electrophysiological recordings, Cx43C271S did not display detectable levels of S-nitrosylation after treatment with DEENO (Fig. 7C). These results confirm that C271 is the critical residue, which is the subject of modification by NO, and is expected to participate in Cx43 hemichannel opening in response to S-nitrosylation in vivo.

DISCUSSION

We previously reported overexpression and pathological remodeling of Cx43 in the hearts of DMD patients and *Dmd*^{mdx} mice (16). β-adrenergic stimulation with Iso caused severe arrhythmias and sudden death in a *Dmd*^{mdx} mice which were prevented by either administration of Cx43 hemichannels blockers or genetically reducing Cx43 protein levels (16, 18). In the present study, we examined cellular and molecular mechanisms by which Cx43 proteins mediates cardiac stress-evoked arrhythmias. We established that β-adrenergic stimulation with Iso promotes changes in membrane permeability and TAs in *Dmd*^{mdx} cardiomyocytes via opening of lateralized and S-nitrosylated Cx43 hemichannels. Normalization of the S-nitrosylation–redox balance by inhibition of the NO synthases reversed changes in membrane permeability, halted TAs and

prevented arrhythmogenic behavior in the *Dmd*^{mdx} mice. Finally, we demonstrated that S-nitrosylation at the residue C271 promotes opening of Cx43 hemichannels. This is a strong indication of a critical role of S-nitrosylated lateralized Cx43 hemichannels in the developing of arrhythmias in *Dmd*^{mdx} mice.

β-adrenergic induced arrhythmias in *Dmd*^{mdx} mice progress over time from premature ventricular contractions to ventricular tachycardia and atrioventricular block (16, 18). These arrhythmic events did not arise as an autonomic defect, such as parasympathetic surge since they were also observed in isolated *Dmd*^{mdx} hearts perfused with Iso (18). Our data suggest that β-adrenergic-induced ventricular arrhythmias are primarily evoked by TA and increased activity of Cx43 hemichannels. It is well known that TA can culminate in sustained abnormal heart rhythms due to early and delayed afterdepolarizations (EAD and DAD, respectively), which are associated with membrane potential oscillations after the upstroke of an action potential (41-43). β-adrenergic stimulation depolarizes the plasma membrane in both WT and *Dmd*^{mdx} (10). However, membrane depolarization in *Dmd*^{mdx} cardiomyocytes was significantly greater and sufficient to promote TAs. Application of Cx43 hemichannels blockers restored the resting membrane potential in Iso treated *Dmd*^{mdx} cardiomyocytes to WT levels and significantly decreased TAs. Our data rule out the role of NCX transporters, which has been implicated in the generation of DADs and arrhythmias in other cardiac pathologies (22-24). This is also in line with previous studies indicating that β-adrenergic stimulation did not activate NCX current under normal condition in the guinea pig, mouse, and rat ventricular myocytes (44). In addition, K^+ currents, which maintained and restored resting membrane potentials followed AP generation, were not affected by the Cx43 hemichannel blocker, Gap19 in both WT and *Dmd*^{mdx} cardiomyocytes (Figure S7).

Our above data indicate that Iso depolarizes *Vm* and produces TAs mainly via Cx43 hemichannel

activity. This idea is further supported by measurements of ethidium uptake across the plasma membrane of intact hearts. Iso-treatment substantially increased membrane permeability in *Dmd*^{mdx} but not WT hearts, which nicely correlates with our findings of significant changes in the membrane potential and the presence of TAs in isolated *Dmd*^{mdx} but not WT cardiomyocytes. Hearts from 4-5 months old *Dmd*^{mdx} mice displayed abnormal membrane permeability, but cardiac dysfunction was undetectable unless mice were subjected to cardiac stress. Because cardiac pathology does not emerge until *Dmd*^{mdx} mice are at least 8 months old, the increase in the membrane permeability might serve as an early sign of DMD cardiomyopathy.

The high conductance and poor selectivity of Cx43 hemichannels (27) combined with increased levels of lateralized Cx43 hemichannels in *Dmd*^{mdx} cardiomyocytes should cause severe membrane depolarizations if Cx43 hemichannels are fully open. However, we only observed a rightward shift of 6 to 8 mV in *Vm* in Iso treated *Dmd*^{mdx} cardiomyocytes compared to WT cells. The latter suggests that Cx43 hemichannel open probability (and/or conductance) is only slightly increased by Iso treatment. Greater increase in open probability of remodeled Cx43 hemichannels could lead to complete collapse of the electrochemical gradient and cell death (45). Cx43 hemichannel function is tightly regulated by physiological extracellular calcium concentrations (46). In line with this, we found that changes in *Vm* in oocytes expressing Cx43 strongly correlate with extracellular calcium concentrations (Fig 6D). Thus, extracellular calcium concentrations in our experiments could limit changes in *Vm* in *Dmd*^{mdx} cardiomyocytes treated with Iso.

It has been widely reported that Iso treatment in isolated cardiomyocytes promotes posttranslational modification (i.e. phosphorylation and S-nitrosylation) of various other cardiac ion channels and transporters, which consequently affect the kinetics of the action potentials (47, 48). Interestingly, we observed that Iso-induced AP prolongation in both WT and *Dmd*^{mdx}

cardiomyocytes was inhibited by Gap19 and AbCx43, suggesting a role for Cx43 hemichannels in sustaining AP prolongation (Figure S8). Interestingly, unpaired Cx43 hemichannels are found at the intercalated disk previous formation to gap junction in a region known as the perinexus (49-51), thus it is possible that Cx43 hemichannels play a role in the setting the local membrane potentials upon physiological conditions. In pathology, however, overexpression and lateralization may exacerbate their activity and create DADs and TAs. Further experiments are necessary to investigate.

When we assessed K^+ currents mediated mainly by voltage-gated potassium (Kv1) and inwardly rectifying K^+ (Kir) currents (52-54), being these last currents those that maintain the *Vm* in several cardiac cells (52, 53, 55, 56), WT and *Dmd*^{mdx} cardiomyocytes displayed similar reversal membrane potential in the presence or absence of Iso (Fig. S7B). In addition, Gap19 did not alter K^+ current reversal potentials in WT and *Dmd*^{mdx} cardiomyocytes. These suggest that K^+ channels did not mediate changes in the resting membrane potential detected in WT and *Dmd*^{mdx} cardiomyocytes upon β-adrenergic stress.

Recent studies indicate that β-adrenergic signaling promotes nitric oxide (NO) production in cardiomyocytes (30, 57-59). In addition to the canonical pathway of NO-induced protein kinase G activation, NO also induces direct post-translational modification of thiol groups in specific cysteine residues on various proteins via S-nitrosylation (60). S-nitrosylation of several Ca^{2+}-handling proteins, including ryanodine receptor (RyR), SERCA2 associated phospholamban (PLB), sodium-calcium exchanger (NCX) and Troponin-C (30, 31, 61), are promoted by β-adrenergic receptors activation. In the DMD heart, the expression of neuronal (nNOS) and

endothelial NO (eNOS) synthases is reduced (62); however, there is a significant increase in the levels of inducible NO (iNOS) synthase (10, 62). This can result in a significant increase in NO production since the iNOS catalytic activity is 100-1000 times higher than that of eNOS and nNOS(63). Several studies suggest that the S-nitrosylation–redox balance might play a key role in ventricular arrhythmias in *Dmd*^{mdx} mice (10, 64, 65). In particular, Fauconnier et al., showed that RyR2 channels from *Dmd*^{mdx} hearts were S-nitrosylated and depleted of calstabin2 (FKBP12.6), resulting in "leaky" RyR2 channels and increased diastolic SR Ca^{2+} leak. Inhibition of SR Ca^{2+} leak prevents membrane depolarization, DADs, and arrhythmias in dystrophic mice (10). The molecular mediators by which leaky RyRs promote membrane depolarization in dystrophic cardiomyocytes have not been investigated.-Recent work indicates that an increase in intracellular Ca^{2+} concentration (up to ~ 500 nM) activates Cx43 hemichannels in both heterologous expression systems and ventricular cardiomyocytes (66). Combined with our results, these findings suggest a causal link between increased SR Ca^{2+} leak and Cx43 hemichannels activation in mediating membrane depolarization and arrhythmias in Iso treated *Dmd*^{mdx} cardiomyocytes and mice, respectively.

S-nitrosylation may also be a potential regulator of Cx43 hemichannels in *Dmd*^{mdx} cardiomyocytes. We found that the level of S-nitrosylated Cx43 is significantly higher in *Dmd*^{mdx} compared to WT hearts. Under resting conditions, *Dmd*^{mdx} and WT cardiomyocytes display S-nitrosylated Cx43 proteins mainly at the intercalated disk regions where they are likely formed gap junction channels. Upon stimulation with Iso, most of the S-nitrosylated Cx43 was found at lateralized regions of *Dmd*^{mdx} cardiomyocytes, where Cx43 is remodeled and primarily forming hemichannels. In contrast, S-nitrosylated Cx43 remained at the disks in WT cells. Consistent with a possible pathophysiological role of S-nitrosylated Cx43 in DMD, hearts from DMD patients

displayed significantly higher levels of S-nitrosylated Cx43 compared to hearts of healthy individuals. Moreover, while S-nitrosylated Cx43 molecules were mostly lateralized in DMD cardiac tissue, they were confined to intercalated disks in hearts of healthy humans.

Inhibition of NO production with L-NAME prevented Iso-induced S-nitrosylation of Cx43 protein. It also prevented increases in membrane permeability and excitability in *Dmd*^{mdx} cardiomyocytes, which in agreement with an absence of arrhythmogenic behavior in *Dmd*^{mdx} mice treated with Iso. To our knowledge, there is no previous evidence indicating that NO inhibition attenuates cardiac stress-induced arrhythmias in the dystrophic mice. We propose that an increase in NO production and consequent S-nitrosylation of lateralized Cx43 hemichannels trigger arrhythmias in *Dmd*^{mdx} mice. In line with this, exogenous administration of NO promoted membrane depolarization and TAs in *Dmd*^{mdx} but not in WT cardiomyocytes via activation of Cx43 hemichannels. Importantly, we also rule out that, in addition to S-nitrosylation of Cx43, the canonical NO-GMPc-PKG pathway is involved in the activation of Cx43 hemichannels. For example, we found that membrane depolarization and TAs in *Dmd*^{mdx} were not affected by ODQ and KT 5823, an inhibitor of soluble guanidyl cyclase and protein kinase G, respectively (Fig. S9A). Consistently, ODQ or KT 5823 did not affect NO-induced Cx43 hemichannel currents in Xenopus oocytes expressing Cx43 (Fig. S9B).

Electrophysiological studies of hemichannels in *Xenopus* oocytes confirmed that NO promotes their opening, and consequently, leads to membrane depolarization. At the molecular level, we found that the Cx43 CT domain is critical for the modification of remodeled hemichannel gating by NO. We identified residue C271 located within this domain as the unique S-nitrosylation site and for the first time demonstrated that S-nitrosylation of C271 is critical for

NO-induced Cx43 hemichannels opening. This is consistent with a previous report identifying C271 as the site for nitrosylation of Cx43 forming gap junction channels (67).

Cx43 remodeling is observed in multiples cardiac pathologies including ischemia, myocardial infarction, hypertrophy and has been linked to arrhythmogenesis due to the reduction of electrical coupling through gap junctions (17, 68-73). It is proposed that reduced electrical coupling slows conduction and favors reentrant excitation resulting in arrhythmias (68-73). However, this is not likely to underlie arrhythmic behaviors observed in DMD hearts where there is no reduction in total Cx43 protein levels (and thus coupling) is detected (18). However, biotin assays experiments suggest that remodeled Cx43 proteins found in dystrophic hearts form undocked hemichannels, and not *de novo* gap junction channels. Compelling evidence indicates that biotin does not bind to Cx43 molecules that are part of gap junction (32, 74). Furthermore, functional and stable Cx43 gap junction channels requires a formation of molecular complex consisting of several intracellular binding proteins, which were not found in association with lateralized Cx43 protein (49). Thus, remodeled lateralized Cx43 hemichannels rather than Cx43 junctional proteins are likely playing a significant role in DMD arrhythmogenesis.

Overall, by supporting a role for Cx43 hemichannels in the development of arrhythmias, our results suggest a significant impact of Cx43 remodeling in other cardiac pathologies, including myocardial infarction and hypertrophy. Cx43 hemichannels emerge as new players that critically affect membrane excitability of *Dmd*^{mdx} cardiomyocytes and promote arrhythmias during β-adrenergic induced cardiac stress. Thus, Cx43 hemichannels could serve as a novel therapeutic target that can prevent cardiac arrhythmias and heart dysfunction.

Materials and methods

Cell Isolation: Ventricular myocytes were enzymatically isolated from mouse hearts (WT and *Dmd*^{mdx}). Mice were heparinized (5000 U/kg) and then anesthetized with overdosed isoflurane, the hearts were removed and were retrogradely perfused at 37 °C in Langendorff fashion with nominally Ca^{2+}-free Tyrode's solution containing 0.5 mg/ml collagenase (Type II; Worthington, Lakewood, NJ, USA) and 0.1 mg/ml protease (type XIV; Sigma, St. Louis, MO, USA) for 10 min. Ca^{2+}-free Tyrode's solution containing (in mM) 136 NaCl, 5.4 KCl, 0.33 Na_2PO_4, 1 $MgCl_2$, 10 glucose, and 10 HEPES (pH 7.4, adjusted with NaOH). The enzyme solution was then washed out, and the hearts were removed from the perfusion apparatus. Left ventricles were placed in petri dishes and were gently teased apart with forceps. Then, the cardiomyocytes were filtered through nylon mesh. The Ca^{2+} concentration was gradually increased to 1.0 mM, and the cells were stored at room temperature and used within 8 h. Only cells from the left ventricular wall were used.

Electrophysiology: Isolated cardiomyocytes were patch-clamped using the whole-cell configuration of the patch-clamp technique in the current-clamp or the voltage-clamp mode. To record APs, patch pipettes (2–5 MΩ) were filled with an internal solution containing (in mM) 110 K^+-aspartate, 30 KCl, 5 NaCl, 10 HEPES, 0.1 EGTA, 5 Mg-ATP, 5 Na_2-creatine phosphate (pH 7.2, adjusted with KOH). The myocytes were superfused with normal Tyrode's solution containing (in mM) 136 NaCl, 5.4 KCl, 0.33 Na_2PO_4, 1.0 $CaCl_2$, 1 $MgCl_2$, 10 glucose, and 10 HEPES (pH 7.4, adjusted with NaOH). Action potentials (APs) were elicited with 2-ms, 2- to 4-nA square pulses at various pacing cycle lengths (PCLs). We quantify triggered activities and changes in the resting membrane potential induced by Iso between 5 and 10 minutes after stimulation. The Gap19 peptide (232ng/µL) and Cx43 antibody (2.5ng/µL) were added in the pipette solution to block

Cx43 hemichannel activity. We used between 2 and 3 cardiomyocytes per each isolated hearts per condition.

The two electro-voltage clamp (TEVC) technique and *Xenopus* oocytes were used to test hemichannel currents from homomeric and heteromeric channels formed by hCx43, hCx26, and hCx26S17F. All connexin clones were purchased from Origene (Rockville, MD, USA). Nhe1-linearized hCx43, hCx26 and hCx26S17F DNA were transcribed in vitro to cRNAs using the T7 Message Machine kit (Ambion, Austin, TX, USA). Electrophysiological data were collected using the Pclamp10 software. All recordings were made at room temperature (20-22ºC). For Cx43 expressing oocytes, the recording solutions contained (mM) 117 TEA and 5 HEPES and 0.2 mM extracellular Ca^{2+} concentration (pH 7.4, adjusted with N-Methyl-D-glucamine). The recording solutions for Cx43Cx26S17F heteromeric hemichannels contained (mM) 118 NaCl, 2 KCl, and 5 HEPES and 1.8 mM of extracellular Ca^{2+} concentration (pH 7.4, adjusted with NaOH). Currents from oocytes were recorded 2 days after cRNA injection, using a Warner OC-725 amplifier (Warner Instruments, USA). Currents were sampled at 2 kHz and low pass filtered as 0.5 kHz. Microelectrode resistances were between 0.1 and 1.2 MΩ when filled with 3M KCl. Antisense oligonucleotides against Cx38 was injected to each oocyte to reduce the expression of endogenous Cx38 at 4 h after harvesting the oocytes (1mg/ml; using the sequence from Ebihara (75)). We assessed hemichannel currents and changes in the resting membrane potential evoked by NO at 10 minutes after stimulation. We used at least three oocytes per each independent frog.

Electrocardiography: Whole animal electrocardiograms (ECGs) were recorded using needle electrodes in a Lead II conformation. Animals were anesthetized by Avertin (2,2,2-tribromoethanol, 290mg/ kg IP) and kept at a constant 37° temperature using a heating pad for the duration of analysis. For inhibition of NO production, animals were treated for one week with

2mM L-NAME (Sigma, St. Louis, MO, USA) via water solution. Following treatment time, mice were tested with isoproterenol (Iso 5mg/kg IP). ECGs were recorded before (baseline line) and after Iso treatment. Arrhythmias were scored based on a point system where: 0= no arrhythmias, 1= single premature ventricular contractions (PVCs), 2= double PVCs, 3= non-sustained ventricular tachycardia (VT), 4= sustained VT or atrioventricular (AV) block, and 5= death. We used between 6 and 7 independents mice per experiments.

Dye perfusion and uptake in isolated hearts: Mice were heparinized (5000 Units/kg) and then anesthetized with Avertin (2,2,2-tribromoethanol, 290 mg/kg, IP). Once unconscious, mice were then injected with either saline (control) or Iso (5 mg/kg, IP). Twenty minutes following Iso or vehicle injection, mice were sacrificed, and hearts were extracted and cannulated in a Langendorff perfusion system. Hearts were perfused with Normal tyrode's buffer (NT) [in mM: 136 NaCl, 5.4 KCl, 0.33 NaH_2PO_4, 1 $MgCl_2$, 1$CaCl_2$, 10 Hepes and 10 Glucose] at 37 °C degrees for 10 minutes, NT containing ethidium bromide (5 µM) or propidium iodide (50 µM) for 20 minutes and then NT buffer for 5 minutes to wash out the dye. Hearts were then fixed overnight in 4% paraformaldehyde (Sigma, St. Louis, MO, USA), placed into 30% sucrose solution in PBS (Sigma, St. Louis, MO, USA) for 12 hours, then embedded in O.C.T (Tissue-Tek, USA). Subsequently 10 µm cryosections were made, slides were thawed to room temperature, washed in PBS and Alexa Fluor Wheat Germ Agglutinin 488 (Invitrogen, NY, USA) was applied for 20 minutes. Slides were then washed in PBS and mounted with mounting reagent with DAPI (Invitrogen, NY, USA). Slides were then imaged using a 200 Axiovert fluorescence microscope (Zeiss, Oberkochen, Germany). To calculate ethidium fluorescence in ImageJ, DAPI stained nuclei were identified, created as ROI and individual nuclei (100-150 per image) mean fluorescent intensities were measured. Then, the ROI outlines were projected onto corresponding ethidium image, where individual fluorescent

intensities were measured, capturing ethidium signal within all nuclei. Ethidium intensity was then divided by DAPI nuclei intensity per each respective ROI signal, then the mean ratio was calculated for all nuclei in the image. We used 6 independent hearts per experiment. In addition, three images per heart were evaluated in a blinded manner.

Biotin Perfusion of Isolated Hearts: Mice were heparinized and then anesthetized with Avertin (2,2,2-tribromoethanol, 290 mg/kg, IP). Once unconscious, mice were sacrificed and hearts were extracted and cannulated in a Langedorff perfusion system. Hearts were initially perfused with NT for 5 minutes, switched to NT buffer plus Biotin (EZ-Link NHS Biotin, 0.5 mg/mL, Thermo Scientific, Waltham, MA, USA) for 60 minutes (0.25 ml/min flow rate) and washed out for 10 minutes with NT buffer plus 15 mM Glycine. Left ventricular tissue was then homogenized in HEN buffer (in mM: 250 HEPES, 1 EDTA, 0.1 Neocuproine, pH 7.7) with 2x HALT protease inhibitors (Thermo Scientific, NY, USA) and then centrifuged at 16,000 g for 10 minutes. Following protein concentration determination, 50 µl of streptavidin beads (Thermo Scientific, NY, USA) were added to 200 µg protein and nutated for 90 minutes at 4^0C with occasional vortexing. Samples were then centrifuged at 16,000 g for 2 minutes, and the supernatant was discarded. The streptavidin pellet was then resuspended in fresh lysis buffer containing 0.1% Triton X-100 and centrifuged for 1 minute at 16,000 g. The pellet was then washed with PBS (pH 7.4) and centrifuged. 25µl of 2x Laemmli sample buffer was added and heated at 100 ^{0}C for 5 minutes to disrupt biotin-streptavidin interaction. The heated samples along were then centrifuged for 1 minute at 16,000 g and the supernatant was run along with total protein extracts without streptavidin pulldown on SDS-PAGE.

Immunofluorescence: Mouse ventricular tissue were frozen in O.C.T (Tissue-Tek, USA). Cryosections were cut at 6µm, slides were thawed to room temperature, washed in PBS for 10

551 minutes and blocked for 1 hour at room temperature with 10% normal donkey serum (Jackson
552 immunoresearch, West Grove, PA, USA) in PBSt wash buffer (PBS + 0.1% Tween20). Sections
553 were then incubated with either N-Cadherin (Invitrogen, NY, USA, #33-3900, 1:200, mouse) and
554 Biotin (Abcam, Cambridge, MA, USA, # ab53494, 1:200, rabbit) antibodies in blocking buffer
555 overnight at 4^0C. Following 3 washes in PBSt, sections were incubated for an hour at room
556 temperature with Alexa Fluor secondary antibodies (Jackson immunoresearch, West Grove, PA,
557 USA) in blocking buffer (1:200). Slides were subsequently washed in PBSt and coverslips were
558 mounted using ProLong gold antifade reagent containing Wheat Germ Agglutinin (WGA), Alexa
559 Fluor™ 350 Conjugate (Thermo Scientific, Waltham, MA, USA). Sections were imaged on a 200
560 Axiovert fluorescence microscope (Zeiss, Oberkochen, Germany).

561 **Western Blotting:** Protein samples from the left ventricular heart wall or from injected Xenopus
562 oocytes were separated by 10% SDS-PAGE and transferred onto a PVDF membrane (BioRad,
563 Hercules, CA, USA). The primary Cx43 (Sigma St. Louis, MO, USA, #C8093, 1:2000, mouse),
564 eNOS (Thermo Scientific, Waltham, MA, USA, #9D10, 1:1000, mouse) and N-Cadherine
565 (Invitrogen, NY, USA, #33-3900; 1:2000, mouse) antibodies and secondary antibodies (Pierce,
566 Rockford, IL, USA; 1/5000) were incubated using the Signal Enhancer HIKARI (Nacalai Tesque,
567 INC, Japan) and the protein bands were detected with the SuperSignal® West Femto (Pierce,
568 Rockford, IL, USA). Molecular mass was estimated with pre-stained markers (BioRad, Hercules,
569 CA, USA). Protein bands were analyzed using the ImageJ software (NIH, USA). We used 6
570 independent hearts per treatment.

571 **Detection of S-nitrosylated proteins:** S-nitrosylated proteins were isolated from either mice heart
572 ventricular samples or Xenopus oocytes expressing Cx43 WT or mutant hemichannels. Heart
573 tissue or Xenopus oocytes were homogenized in HEN buffer (in mM: 250 HEPES, 1 EDTA, 0.1

Neucoproine, pH 7.7) containing protease inhibitors. Samples containing 200 μg protein were treated by the biotin-switch method to pull down all S-nitrosylated proteins (76). Briefly, samples were incubated with methyl methanethiosulfonate reagents (MMTS, Sigma, St. Louis, MO, USA) for 1-h at 50°C in the dark to block cysteine free thiols (-SH). After, proteins were precipitated with four volumes of ice-cold acetone, repeatedly washed with acetone to remove free MMTS and resolubilized. Thereafter, nitrosylated cysteine residues (-S-NO) were reduced to free cysteine by incubating 1-hour with 30mM sodium ascorbate (Sigma, St. Louis, MO, USA) and labeled with HPDP-biotin (Thermo Scientific, Waltham, MA, USA). Proteins were precipitated with acetone to wash the excess of HPDP-biotin and solubilized for Western blot analysis. Following solubilization, the samples were incubated 1-hour with agarose-conjugated streptavidin beads (Thermo Scientific, Waltham, MA, USA) and centrifuged to pull-down HPDP-biotinylated proteins. Adsorbed proteins were separated using 10% SDS-PAGE and transferred onto a PVDF membrane (BioRad, Hercules, CA, USA). A monoclonal anti-Cx43 (Sigma, St. Louis, MO, USA, #C8093, 1:2000, mouse) was used to detect Cx43 protein. For all Western blot analysis, the intensity of the signal was evaluated using the Image J program (NIH, USA). We used 6 independent hearts per treatment.

Analysis of protein-to-protein association: The subcellular distribution and possible spatial association between S-NO and Cx43 were evaluated by Proximity Ligation Assay(77) (Sigma, St. Louis, MO, USA). Tissue sections (6 μm) were blocked and incubated with two primary antibodies from different species, which were, then, detected using oligonucleotide-conjugated secondary antibodies as described in the manufacturer's protocols. The antibodies used were a monoclonal anti-Cx43 (Sigma, St. Louis, MO, USA, #C8093, 1:200) and an anti-S-nitrosocysteine antibody (Sigma, St. Louis, MO, USA, #N5411, 1:100). If the target proteins are closer than 20

nm, the oligonucleotides can be used as template for DNA ligase-mediated joining of additional oligonucleotides to form a circular DNA molecule, which was amplified using hybridizing fluorophore-labeled oligonucleotides. Images were visualized with a 200 Axiovert fluorescence microscope (Zeiss, Oberkochen, Germany). We used 5 independent hearts per treatment.

Chemicals: N^{ω}-nitro-L-arginine (L-NAME), HEPES, cAMP, Na_2-creatine phosphate, K^+-aspartate, N-Methyl-D-glucamine and tetraethylammonium (TEA) were purchased from Sigma-Aldrich (St. Louis, MO, USA). Sodium 2-(N, N-diethylamino)-diazenolate-2-oxide (DEENO) and Isoproterenol were obtained from Calbiochem (La Jolla, CA, USA) and collagenase type II from Worthington (Lakewood, NJ, USA). Gap19 was purchased from Tocris (Minneapolis, MN, USA).

Statistical analysis: Values are displayed as mean ± standard error. Comparisons between groups were made using one-way ANOVA or two-way ANOVA plus Tukey post-hoc test, as appropriate. In the case of two groups, we performed paired two tailed Student's t test. $P < 0.05$ was considered significant. Each legend figure indicated the respective *n* value.

STUDY APPROVAL:

Mouse Breeding and Genotyping: WT and *Dmd*^{mdx} male mice were purchased in Jackson Labs and analyzed at time points of 5-6 months. All animal experiments were approved by the IACUC of Rutgers New Jersey Medical School and performed in accordance with the NIH guidelines.

Human Samples: Two non-DMD and two DMD male human heart samples were obtained from the University of Maryland Brain and Tissue Bank, a member of the NIH NeuroBioBank network. All samples were dissected post-mortem. Informed consent was obtained from all subjects from whom tissues were analyzed. All human experiments were approved by the IRB of Rutgers University and performed in accordance with relevant guidelines and regulations.

Acknowledgments: We thank Dr. Theanne Griffith for critically reading the manuscript. **Funding:** This work was supported by an AHA post-doctoral fellowship 18POST339610107 to M.A.L., AHA pre-doctoral fellowship 17PRE33660354 to E.H., a Muscular Dystrophy Association grant 416281 to D.F., NIH grant HL093342 to N.S., NIH grants R01HL92929 and R01Hl133294 to L.H.X., AHA grant 16GRNT31100022 to L.H.X., NIH grant 1R01HL141170-01 to D.F., N.S., J.E.C., and NIH grant 1R01GM099490 to J.E.C.

Author contributions: M.A.L., E.H., D.F, N.S., L.H.X and J.E.C designed experiments. M.A.L. performed most of the experiments. M.A.L, J.E.C., L.H.X, and N.S. analyzed the data. M.A.L and J.E.C wrote the manuscript. E.H and N.S edited the manuscript. All authors reviewed and approved final draft. **Competing Interests:** The authors have no competing interests.

References

1. Davies KE, and Nowak KJ. Molecular mechanisms of muscular dystrophies: old and new players. *Nat Rev Mol Cell Biol.* 2006;7(10):762-73.
2. Hoffman EP, Brown RH, Jr., and Kunkel LM. Dystrophin: the protein product of the Duchenne muscular dystrophy locus. *Cell.* 1987;51(6):919-28.
3. de Kermadec JM, Becane HM, Chenard A, Tertrain F, and Weiss Y. Prevalence of left ventricular systolic dysfunction in Duchenne muscular dystrophy: an echocardiographic study. *American heart journal.* 1994;127(3):618-23.
4. Connuck DM, Sleeper LA, Colan SD, Cox GF, Towbin JA, Lowe AM, et al. Characteristics and outcomes of cardiomyopathy in children with Duchenne or Becker muscular dystrophy: a comparative study from the Pediatric Cardiomyopathy Registry. *American heart journal.* 2008;155(6):998-1005.
5. Hermans MC, Pinto YM, Merkies IS, de Die-Smulders CE, Crijns HJ, and Faber CG. Hereditary muscular dystrophies and the heart. *Neuromuscul Disord.* 2010;20(8):479-92.
6. Bushby K, Finkel R, Birnkrant DJ, Case LE, Clemens PR, Cripe L, et al. Diagnosis and management of Duchenne muscular dystrophy, part 2: implementation of multidisciplinary care. *The Lancet Neurology.* 2010;9(2):177-89.
7. Garg R, and Yusuf S. Overview of randomized trials of angiotensin-converting enzyme inhibitors on mortality and morbidity in patients with heart failure. Collaborative Group on ACE Inhibitor Trials. *Jama.* 1995;273(18):1450-6.
8. Ather S, Wang W, Wang Q, Li N, Anderson ME, and Wehrens XH. Inhibition of CaMKII phosphorylation of RyR2 prevents inducible ventricular arrhythmias in mice with Duchenne muscular dystrophy. *Heart Rhythm.* 2013;10(4):592-9.
9. Kyrychenko S, Polakova E, Kang C, Pocsai K, Ullrich ND, Niggli E, et al. Hierarchical accumulation of RyR post-translational modifications drives disease progression in dystrophic cardiomyopathy. *Cardiovasc Res.* 2013;97(4):666-75.
10. Fauconnier J, Thireau J, Reiken S, Cassan C, Richard S, Matecki S, et al. Leaky RyR2 trigger ventricular arrhythmias in Duchenne muscular dystrophy. *Proc Natl Acad Sci U S A.* 2010;107(4):1559-64.
11. Kleber AG, and Saffitz JE. Role of the intercalated disc in cardiac propagation and arrhythmogenesis. *Frontiers in physiology.* 2014;5:404.
12. Gros DB, and Jongsma HJ. Connexins in mammalian heart function. *BioEssays : news and reviews in molecular, cellular and developmental biology.* 1996;18(9):719-30.
13. Severs NJ, Coppen SR, Dupont E, Yeh HI, Ko YS, and Matsushita T. Gap junction alterations in human cardiac disease. *Cardiovasc Res.* 2004;62(2):368-77.
14. Severs NJ, Dupont E, Coppen SR, Halliday D, Inett E, Baylis D, et al. Remodelling of gap junctions and connexin expression in heart disease. *Biochimica et biophysica acta.* 2004;1662(1-2):138-48.
15. Severs NJ, Dupont E, Thomas N, Kaba R, Rothery S, Jain R, et al. Alterations in cardiac connexin expression in cardiomyopathies. *Adv Cardiol.* 2006;42:228-42.
16. Gonzalez JP, Ramachandran J, Xie LH, Contreras JE, and Fraidenraich D. Selective Connexin43 Inhibition Prevents Isoproterenol-Induced Arrhythmias and Lethality in Muscular Dystrophy Mice. *Sci Rep.* 2015;5:13490.

17. Colussi C, Rosati J, Straino S, Spallotta F, Berni R, Stilli D, et al. Nepsilon-lysine acetylation determines dissociation from GAP junctions and lateralization of connexin 43 in normal and dystrophic heart. *Proc Natl Acad Sci U S A.* 2011;108(7):2795-800.
18. Gonzalez JP, Ramachandran J, Himelman E, Badr MA, Kang C, Nouet J, et al. Normalization of connexin 43 protein levels prevents cellular and functional signs of dystrophic cardiomyopathy in mice. *Neuromuscul Disord.* 2018;28(4):361-72.
19. Wasala NB, Bostick B, Yue Y, and Duan D. Exclusive skeletal muscle correction does not modulate dystrophic heart disease in the aged mdx model of Duchenne cardiomyopathy. *Human molecular genetics.* 2013;22(13):2634-41.
20. Abudara V, Bechberger J, Freitas-Andrade M, De Bock M, Wang N, Bultynck G, et al. The connexin43 mimetic peptide Gap19 inhibits hemichannels without altering gap junctional communication in astrocytes. *Frontiers in cellular neuroscience.* 2014;8:306.
21. Wang N, De Vuyst E, Ponsaerts R, Boengler K, Palacios-Prado N, Wauman J, et al. Selective inhibition of Cx43 hemichannels by Gap19 and its impact on myocardial ischemia/reperfusion injury. *Basic Res Cardiol.* 2013;108(1):309.
22. Hegyi B, Morotti S, Liu C, Ginsburg KS, Bossuyt J, Belardinelli L, et al. Enhanced Depolarization Drive in Failing Rabbit Ventricular Myocytes. *Circ Arrhythm Electrophysiol.* 2019;12(3):e007061.
23. Hegyi B, Bossuyt J, Griffiths LG, Shimkunas R, Coulibaly Z, Jian Z, et al. Complex electrophysiological remodeling in postinfarction ischemic heart failure. *Proc Natl Acad Sci U S A.* 2018;115(13):E3036-E44.
24. Sato D, Clancy CE, and Bers DM. Dynamics of sodium current mediated early afterdepolarizations. *Heliyon.* 2017;3(9):e00388.
25. Baczko I, Giles WR, and Light PE. Resting membrane potential regulates Na(+)-Ca2+ exchange-mediated Ca2+ overload during hypoxia-reoxygenation in rat ventricular myocytes. *J Physiol.* 2003;550(Pt 3):889-98.
26. Matsuda T, Arakawa N, Takuma K, Kishida Y, Kawasaki Y, Sakaue M, et al. SEA0400, a novel and selective inhibitor of the Na+-Ca2+ exchanger, attenuates reperfusion injury in the in vitro and in vivo cerebral ischemic models. *J Pharmacol Exp Ther.* 2001;298(1):249-56.
27. Contreras JE, Saez JC, Bukauskas FF, and Bennett MV. Gating and regulation of connexin 43 (Cx43) hemichannels. *Proc Natl Acad Sci U S A.* 2003;100(20):11388-93.
28. Johnson RG, Le HC, Evenson K, Loberg SW, Myslajek TM, Prabhu A, et al. Connexin Hemichannels: Methods for Dye Uptake and Leakage. *The Journal of membrane biology.* 2016;249(6):713-41.
29. Figueroa XF, Lillo MA, Gaete PS, Riquelme MA, and Saez JC. Diffusion of nitric oxide across cell membranes of the vascular wall requires specific connexin-based channels. *Neuropharmacology.* 2013;75:471-8.
30. Irie T, Sips PY, Kai S, Kida K, Ikeda K, Hirai S, et al. S-Nitrosylation of Calcium-Handling Proteins in Cardiac Adrenergic Signaling and Hypertrophy. *Circ Res.* 2015;117(9):793-803.
31. Vielma AZ, Leon L, Fernandez IC, Gonzalez DR, and Boric MP. Nitric Oxide Synthase 1 Modulates Basal and beta-Adrenergic-Stimulated Contractility by Rapid and Reversible Redox-Dependent S-Nitrosylation of the Heart. *PLoS One.* 2016;11(8):e0160813.
32. Retamal MA, Cortes CJ, Reuss L, Bennett MV, and Saez JC. S-nitrosylation and permeation through connexin 43 hemichannels in astrocytes: induction by oxidant stress and reversal by reducing agents. *Proc Natl Acad Sci U S A.* 2006;103(12):4475-80.
33. Pfeiffer S, Leopold E, Schmidt K, Brunner F, and Mayer B. Inhibition of nitric oxide synthesis by NG-nitro-L-arginine methyl ester (L-NAME): requirement for bioactivation to the free acid, NG-nitro-L-arginine. *British journal of pharmacology.* 1996;118(6):1433-40.
34. Garcia IE, Maripillan J, Jara O, Ceriani R, Palacios-Munoz A, Ramachandran J, et al. Keratitis-ichthyosis-deafness syndrome-associated Cx26 mutants produce nonfunctional gap junctions but

hyperactive hemichannels when co-expressed with wild type Cx43. *The Journal of investigative dermatology.* 2015;135(5):1338-47.
35. Hansen DB, Braunstein TH, Nielsen MS, and MacAulay N. Distinct permeation profiles of the connexin 30 and 43 hemichannels. *FEBS letters.* 2014;588(8):1446-57.
36. White TW, Deans MR, O'Brien J, Al-Ubaidi MR, Goodenough DA, Ripps H, et al. Functional characteristics of skate connexin35, a member of the gamma subfamily of connexins expressed in the vertebrate retina. *The European journal of neuroscience.* 1999;11(6):1883-90.
37. Srinivas M, Jannace TF, Cocozzelli AG, Li L, Slavi N, Sellitto C, et al. Connexin43 mutations linked to skin disease have augmented hemichannel activity. *Sci Rep.* 2019;9(1):19.
38. Lampe PD, and Lau AF. The effects of connexin phosphorylation on gap junctional communication. *The international journal of biochemistry & cell biology.* 2004;36(7):1171-86.
39. Laird DW, Puranam KL, and Revel JP. Turnover and phosphorylation dynamics of connexin43 gap junction protein in cultured cardiac myocytes. *The Biochemical journal.* 1991;273(Pt 1):67-72.
40. Solan JL, and Lampe PD. Specific Cx43 phosphorylation events regulate gap junction turnover in vivo. *FEBS letters.* 2014;588(8):1423-9.
41. Marban E, Robinson SW, and Wier WG. Mechanisms of arrhythmogenic delayed and early afterdepolarizations in ferret ventricular muscle. *The Journal of clinical investigation.* 1986;78(5):1185-92.
42. Priori SG, and Corr PB. Mechanisms underlying early and delayed afterdepolarizations induced by catecholamines. *The American journal of physiology.* 1990;258(6 Pt 2):H1796-805.
43. Priori SG, Mantica M, Napolitano C, and Schwartz PJ. Early afterdepolarizations induced in vivo by reperfusion of ischemic myocardium. A possible mechanism for reperfusion arrhythmias. *Circulation.* 1990;81(6):1911-20.
44. Lin X, Jo H, Sakakibara Y, Tambara K, Kim B, Komeda M, et al. Beta-adrenergic stimulation does not activate Na+/Ca2+ exchange current in guinea pig, mouse, and rat ventricular myocytes. *American journal of physiology Cell physiology.* 2006;290(2):C601-8.
45. Laird DW, and Lampe PD. Therapeutic strategies targeting connexins. *Nat Rev Drug Discov.* 2018.
46. Lopez W, Ramachandran J, Alsamarah A, Luo Y, Harris AL, and Contreras JE. Mechanism of gating by calcium in connexin hemichannels. *Proc Natl Acad Sci U S A.* 2016;113(49):E7986-E95.
47. Gomez R, Caballero R, Barana A, Amoros I, Calvo E, Lopez JA, et al. Nitric oxide increases cardiac IK1 by nitrosylation of cysteine 76 of Kir2.1 channels. *Circ Res.* 2009;105(4):383-92.
48. Tamargo J, Caballero R, Gomez R, and Delpon E. Cardiac electrophysiological effects of nitric oxide. *Cardiovasc Res.* 2010;87(4):593-600.
49. Rhett JM, and Gourdie RG. The perinexus: a new feature of Cx43 gap junction organization. *Heart Rhythm.* 2012;9(4):619-23.
50. Rhett JM, Veeraraghavan R, Poelzing S, and Gourdie RG. The perinexus: sign-post on the path to a new model of cardiac conduction? *Trends Cardiovasc Med.* 2013;23(6):222-8.
51. Hoagland DT, Santos W, Poelzing S, and Gourdie RG. The role of the gap junction perinexus in cardiac conduction: Potential as a novel anti-arrhythmic drug target. *Prog Biophys Mol Biol.* 2019;144:41-50.
52. Chilton L, Ohya S, Freed D, George E, Drobic V, Shibukawa Y, et al. K+ currents regulate the resting membrane potential, proliferation, and contractile responses in ventricular fibroblasts and myofibroblasts. *Am J Physiol Heart Circ Physiol.* 2005;288(6):H2931-9.
53. Vandenberg CA. Inward rectification of a potassium channel in cardiac ventricular cells depends on internal magnesium ions. *Proc Natl Acad Sci U S A.* 1987;84(8):2560-4.
54. Yuan XJ. Voltage-gated K+ currents regulate resting membrane potential and [Ca2+]i in pulmonary arterial myocytes. *Circ Res.* 1995;77(2):370-8.

55. Miragoli M, Gaudesius G, and Rohr S. Electrotonic modulation of cardiac impulse conduction by myofibroblasts. *Circ Res.* 2006;98(6):801-10.
56. Reimann F, and Ashcroft FM. Inwardly rectifying potassium channels. *Curr Opin Cell Biol.* 1999;11(4):503-8.
57. Curran J, Tang L, Roof SR, Velmurugan S, Millard A, Shonts S, et al. Nitric oxide-dependent activation of CaMKII increases diastolic sarcoplasmic reticulum calcium release in cardiac myocytes in response to adrenergic stimulation. *PloS one.* 2014;9(2):e87495.
58. Pereira L, Bare DJ, Galice S, Shannon TR, and Bers DM. beta-Adrenergic induced SR Ca(2+) leak is mediated by an Epac-NOS pathway. *J Mol Cell Cardiol.* 2017;108:8-16.
59. Gutierrez DA, Fernandez-Tenorio M, Ogrodnik J, and Niggli E. NO-dependent CaMKII activation during beta-adrenergic stimulation of cardiac muscle. *Cardiovasc Res.* 2013;100(3):392-401.
60. Hess DT, Matsumoto A, Kim SO, Marshall HE, and Stamler JS. Protein S-nitrosylation: purview and parameters. *Nat Rev Mol Cell Biol.* 2005;6(2):150-66.
61. Chung HS, Kim GE, Holewinski RJ, Venkatraman V, Zhu G, Bedja D, et al. Transient receptor potential channel 6 regulates abnormal cardiac S-nitrosylation in Duchenne muscular dystrophy. *Proc Natl Acad Sci U S A.* 2017;114(50):E10763-E71.
62. Bia BL, Cassidy PJ, Young ME, Rafael JA, Leighton B, Davies KE, et al. Decreased myocardial nNOS, increased iNOS and abnormal ECGs in mouse models of Duchenne muscular dystrophy. *J Mol Cell Cardiol.* 1999;31(10):1857-62.
63. MacMicking J, Xie QW, and Nathan C. Nitric oxide and macrophage function. *Annu Rev Immunol.* 1997;15:323-50.
64. Cutler MJ, Plummer BN, Wan X, Sun QA, Hess D, Liu H, et al. Aberrant S-nitrosylation mediates calcium-triggered ventricular arrhythmia in the intact heart. *Proc Natl Acad Sci U S A.* 2012;109(44):18186-91.
65. Gonzalez DR, Beigi F, Treuer AV, and Hare JM. Deficient ryanodine receptor S-nitrosylation increases sarcoplasmic reticulum calcium leak and arrhythmogenesis in cardiomyocytes. *Proc Natl Acad Sci U S A.* 2007;104(51):20612-7.
66. Wang N, De Bock M, Antoons G, Gadicherla AK, Bol M, Decrock E, et al. Connexin mimetic peptides inhibit Cx43 hemichannel opening triggered by voltage and intracellular Ca2+ elevation. *Basic Res Cardiol.* 2012;107(6):304.
67. Straub AC, Billaud M, Johnstone SR, Best AK, Yemen S, Dwyer ST, et al. Compartmentalized connexin 43 s-nitrosylation/denitrosylation regulates heterocellular communication in the vessel wall. *Arterioscler Thromb Vasc Biol.* 2011;31(2):399-407.
68. Yao JA, Hussain W, Patel P, Peters NS, Boyden PA, and Wit AL. Remodeling of gap junctional channel function in epicardial border zone of healing canine infarcts. *Circ Res.* 2003;92(4):437-43.
69. Peters NS, Coromilas J, Severs NJ, and Wit AL. Disturbed connexin43 gap junction distribution correlates with the location of reentrant circuits in the epicardial border zone of healing canine infarcts that cause ventricular tachycardia. *Circulation.* 1997;95(4):988-96.
70. Luke RA, and Saffitz JE. Remodeling of ventricular conduction pathways in healed canine infarct border zones. *J Clin Invest.* 1991;87(5):1594-602.
71. Kleber AG, Riegger CB, and Janse MJ. Electrical uncoupling and increase of extracellular resistance after induction of ischemia in isolated, arterially perfused rabbit papillary muscle. *Circ Res.* 1987;61(2):271-9.
72. Cooklin M, Wallis WR, Sheridan DJ, and Fry CH. Changes in cell-to-cell electrical coupling associated with left ventricular hypertrophy. *Circ Res.* 1997;80(6):765-71.
73. Lin X, Gemel J, Beyer EC, and Veenstra RD. Dynamic model for ventricular junctional conductance during the cardiac action potential. *Am J Physiol Heart Circ Physiol.* 2005;288(3):H1113-23.

74. Musil LS, and Goodenough DA. Biochemical analysis of connexin43 intracellular transport, phosphorylation, and assembly into gap junctional plaques. *J Cell Biol.* 1991;115(5):1357-74.
75. Ebihara L. Xenopus connexin38 forms hemi-gap-junctional channels in the nonjunctional plasma membrane of Xenopus oocytes. *Biophys J.* 1996;71(2):742-8.
76. Jaffrey SR, and Snyder SH. The biotin switch method for the detection of S-nitrosylated proteins. *Sci STKE.* 2001;2001(86):pl1.
77. Soderberg O, Gullberg M, Jarvius M, Ridderstrale K, Leuchowius KJ, Jarvius J, et al. Direct observation of individual endogenous protein complexes in situ by proximity ligation. *Nat Methods.* 2006;3(12):995-1000.

FIGURES

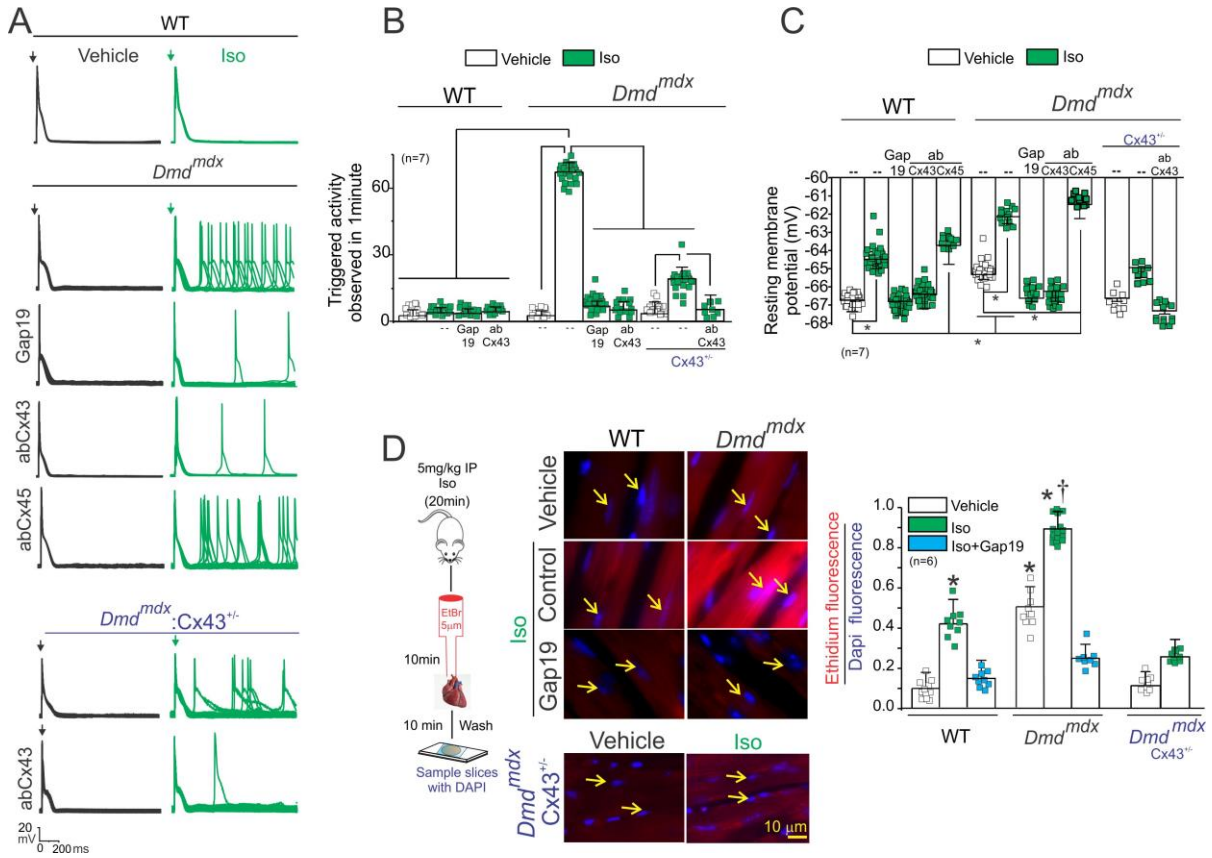

Fig 1. Isoproterenol induces TA in *Dmd*^{mdx} cardiomyocytes via opening of Cx43 hemichannels.

A) Representative action potentials traces of WT, *Dmd*^{mdx} and *Dmd*^{mdx}Cx43$^{+/-}$ isolated cardiomyocytes. Cells were stimulated with 1µM isoproterenol (Iso, green) in the absence or presence of Cx43 or Cx45 hemichannel blockers contained inside the pipette: Gap19 (232ng/µL), Cx43 CT antibody (abCx43; 2.5 ng/µL) or Cx45 CT antibody (2.5 ng/µL). Arrow indicates electrical stimulation pulse. **B)** Quantification of TA induced by Iso observed in **(A)**. Comparisons between groups were made using two-way ANOVA plus Tukey post-hoc test, *P<0.05. **C)** Resting membrane potential of WT and *Dmd*^{mdx} cardiomyocytes. The number in parentheses indicates the *n* value. Comparisons between groups were made using two-way ANOVA plus Tukey post-hoc test, *P<0.05. **D)** Assessment of Cx43 hemichannel activity in the whole heart via ethidium uptake. Isolated hearts were perfused with buffer containing 5µM ethidium after vehicle or Iso (5mg/kg, IP). The number in parentheses indicates the *n* value. Comparisons between groups were made using two-way ANOVA plus Tukey post-hoc test. *P<0.05 vs Vehicle WT, †P<0.05 vs Vehicle *Dmd*^{mdx}.

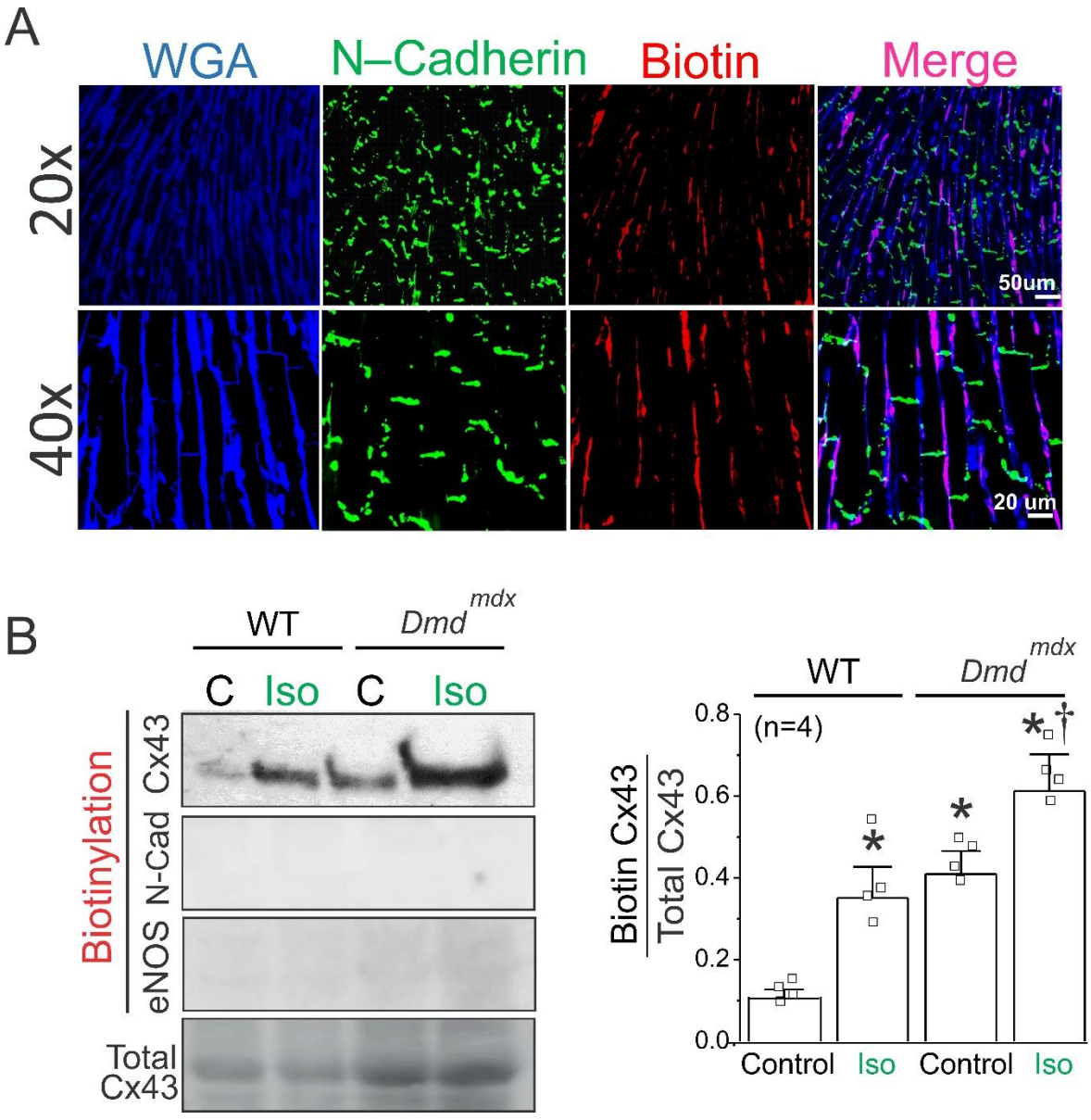

Fig 2. Biotin perfused in intact hearts interact only with plasma membrane of cardiomyocytes at the lateral side.

A) Representative immunofluorescence against N-cadherin (green) and biotin (red) in a *Dmd*^{mdx} heart sample. Biotin was perfused for 60 minutes before heart fixation. Cryosections were stained with wheat germ agglutinin (WGA, blue). Note that biotin was only positively stained at the lateral borders of cardiomyocytes and not at IDs. **B)** Western blot analysis (left) and quantification (right) of Cx43 from biotin perfused hearts (biotinylation). Bottom row represents Cx43-immunoblotted samples from heart lysates prior to pulldown (total Cx43). Biotinylated Cx43 levels were expressed as fold change relative to total Cx43 protein levels per sample. Note that biotin did not interact with intracellular proteins (eNOS) and intercalated disk proteins (N-Cadherin). The number in parentheses indicates the *n* value. Comparisons between groups were made using two-way ANOVA plus Tukey post-hoc test. *P<0.05 vs WT control, †<0.05 vs *Dmd*^{mdx} control.

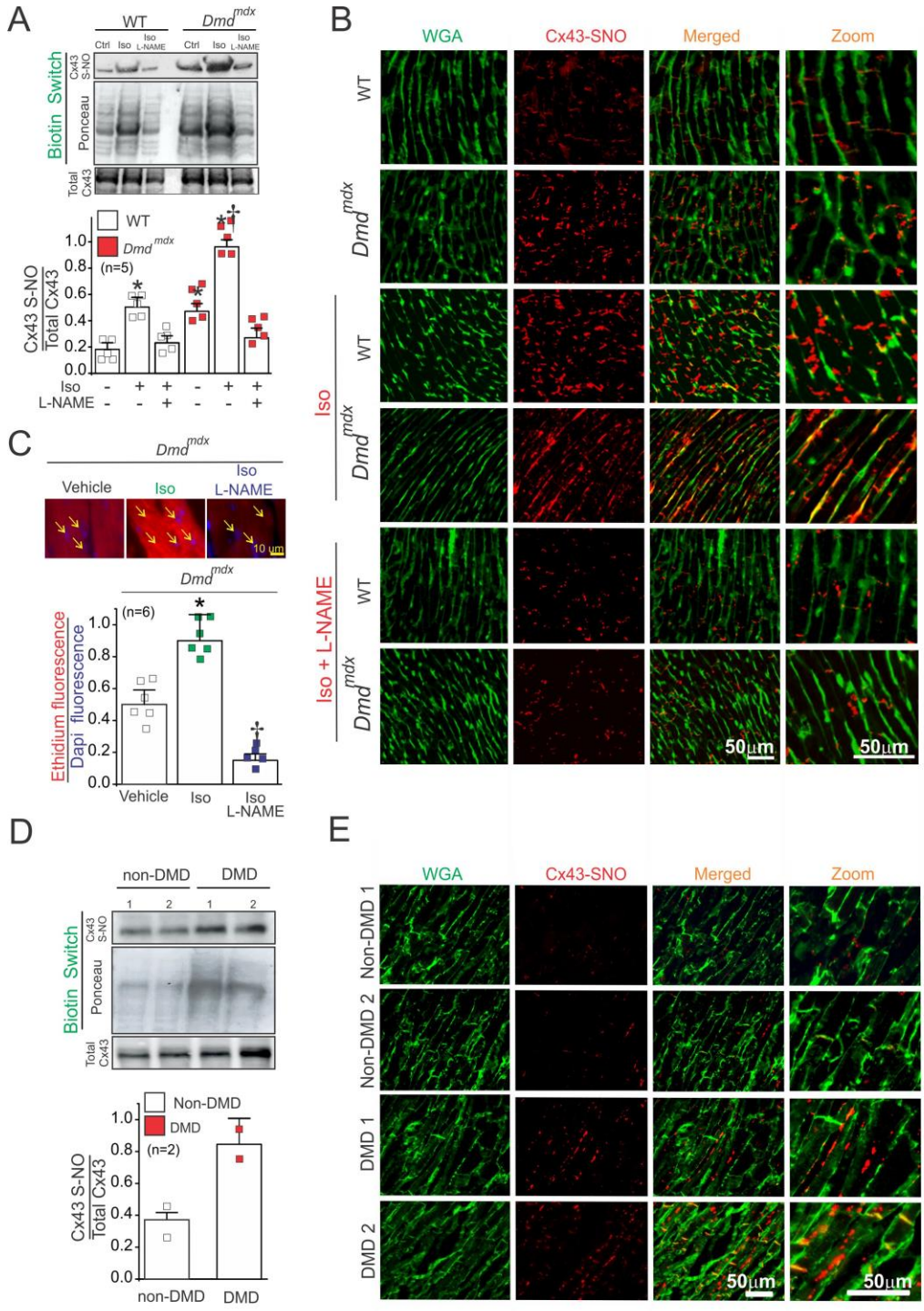
A
WT
Dmd mdx
Ctrl Iso Iso L-NAME
Biotin Switch
Cx43 S-NO
Ponceau
Total Cx43
WT
Dmd mdx
(n=5)
Cx43 S-NO / Total Cx43
Iso
L-NAME
B
WGA
Cx43-SNO
Merged
Zoom
WT
Dmd mdx
Iso
Iso + L-NAME
50µm
C
Dmd mdx
Vehicle
Iso
Iso L-NAME
10 µm
(n=6)
Ethidium fluorescence / Dapi fluorescence
Vehicle
Iso
Iso L-NAME
D
non-DMD
DMD
Biotin Switch
Cx43 S-NO
Ponceau
Total Cx43
Non-DMD
DMD
(n=2)
Cx43 S-NO / Total Cx43
non-DMD
DMD
E
WGA
Cx43-SNO
Merged
Zoom
Non-DMD 1
Non-DMD 2
DMD 1
DMD 2
50µm

Fig 3. Isoproterenol increases S-nitrosylated levels of Cx43 at the lateral side of *Dmd*^{mdx} cardiomyocytes.

A) Top and middle gels were loaded with S-nitrosylated proteins pulled down from heart samples using the biotin switch assay. Top gel was, then, blot against Cx43 and the middle gel is the corresponding ponceau staining. Lower blot was load using total cardiac proteins and blot against Cx43. The bottom graph is the quantification for 5 independent blots using the ratio for SNO-Cx43/Ponceau. The number in parentheses indicates the *n* value. Comparisons between groups were made using two-way ANOVA plus Tukey post-hoc test. *P<0.05 vs WT control, †<0.05 vs WT Iso. **B)** Analysis performed by Proximity Ligation assay (PLA) of the interaction between Cx43 and S-nitrosylation. Plasma membrane stained with wheat germ agglutinin (WGA) and S-nitrosylated Cx43 (Cx43-SNO) are shown in green and red, respectively. Representative images of n = 5 per group. **C)** Assessment of Cx43 hemichannel activity in isolated *Dmd*^{mdx} hearts perfused with buffer containing 5μM ethidium bromide after or not treatment with Iso. The number in parentheses indicates the *n* value. Comparisons between groups were made using two-way ANOVA test plus Tukey post-hoc test. *P<0.05 vs Vehicle WT, †P<0.05 vs Vehicle *Dmd*^{mdx}. **D)** Top and middle gels were loaded with S-nitrosylated proteins pulled down from human heart samples using the biotin switch assay. Top gel was, then, blot against Cx43 and the middle gel is the corresponding ponceau staining. Lower blot was load using total cardiac proteins and blot against Cx43. **E)** Analysis performed by Proximity Ligation assay (PLA) of the interaction between Cx43 and S-nitrosylation in human samples. Note that, Cx43 is S-nitrosylated at the lateral side of DMD human samples compare to non-DMD.

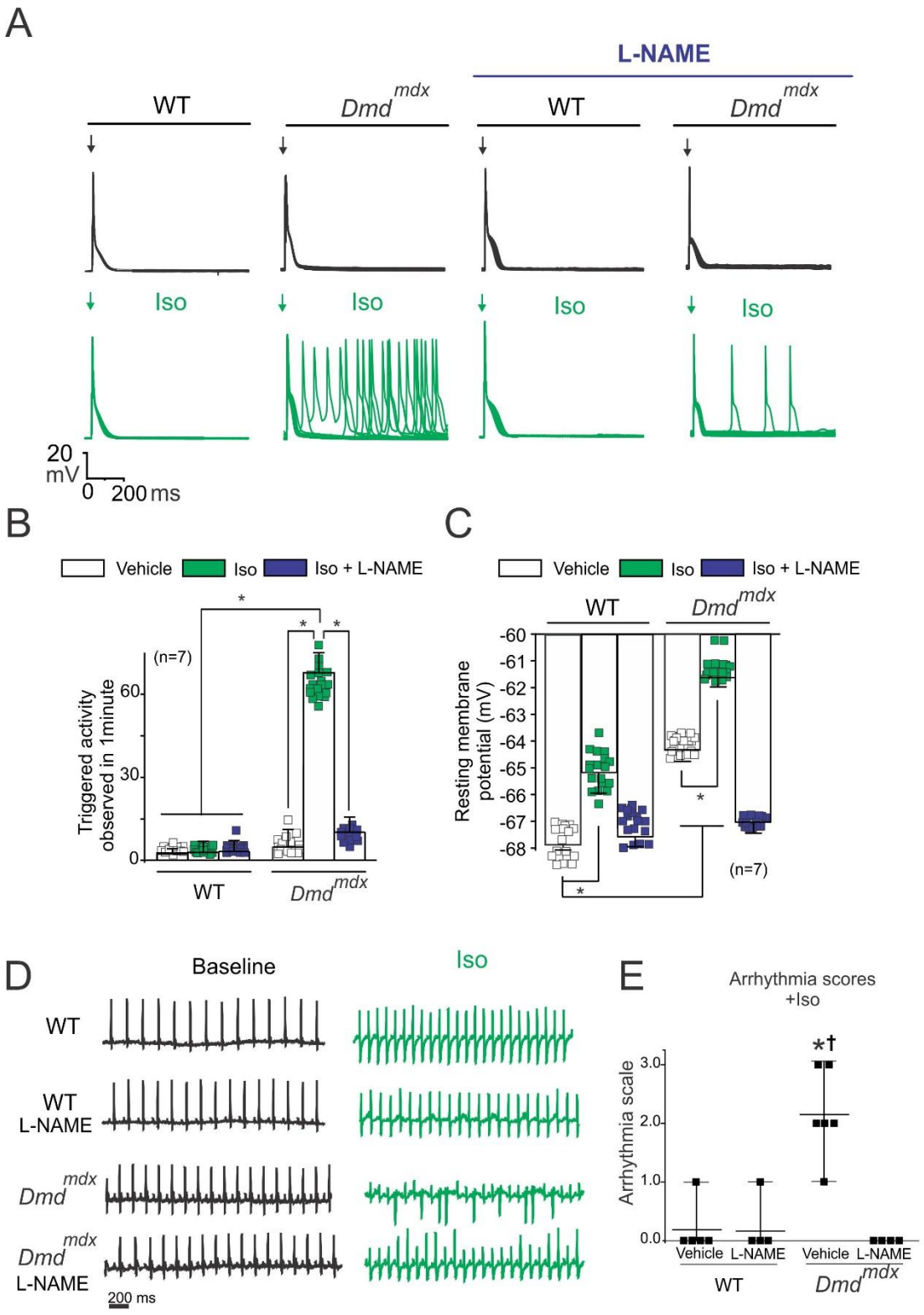
A
L-NAME
WT
Dmd mdx
WT
Dmd mdx
Iso
Iso
Iso
Iso
20 mV
0 200 ms
B
Vehicle
Iso
Iso + L-NAME
Triggered activity observed in 1minute
(n=7)
60
30
0
WT
Dmd mdx
C
Vehicle
Iso
Iso + L-NAME
WT
Dmd mdx
Resting membrane potential (mV)
-60
-61
-62
-63
-64
-65
-66
-67
-68
(n=7)
D
Baseline
Iso
WT
WT L-NAME
Dmd mdx
Dmd mdx L-NAME
200 ms
E
Arrhythmia scores +Iso
Arrhythmia scale
3.0
2.0
1.0
0.0
Vehicle
L-NAME
Vehicle
L-NAME
WT
Dmd mdx

Fig 4. Blockade of nitric oxide production prevents Cx43 hemichannels mediated TA and arrhythmias in *Dmd*^{mdx} mice.

A) Representative action potentials traces of WT and *Dmd*^{mdx} isolated cardiomyocytes. Cells were stimulated with 1μM isoproterenol (Iso) in the presence of 100μM L-NAME. Arrow indicates electrical stimulation. **B)** Quantification of TA induced by Iso observed in **(A)**. The number in parentheses indicates the *n* value. Comparisons between groups were made using two-way ANOVA plus Tukey post-hoc test *P<0.05.**C)** Resting membrane potential of WT and *Dmd*^{mdx} cardiomyocytes. Comparisons between groups were made using two-way ANOVA plus Tukey post-hoc test. **D)** Representative ECG traces of 5 to 6 month-old WT and *Dmd*^{mdx} mice that were previously treated or not with 2 mM L-NAME (an unspecific NOS blocker) via drinking water. EGC baseline (left) and EGC after Iso treatment (5mg/kg, IP) are shown for comparison. **E)** Arrhythmia score based on pre-determined scale where 0 = no arrhythmias, 1 = single PVCs, 2 = double PVCs, 3 = triple PVCs or non-sustained VT, 4 = sustained VT or AV block, 5 = death. * p<0.0001 versus WT; †p <0.0001 versus *Dmd*^{mdx} L-NAME. The number in parentheses indicates the *n* value. Statistical significance determined by 1-way ANOVA plus Tukey post-hoc test.

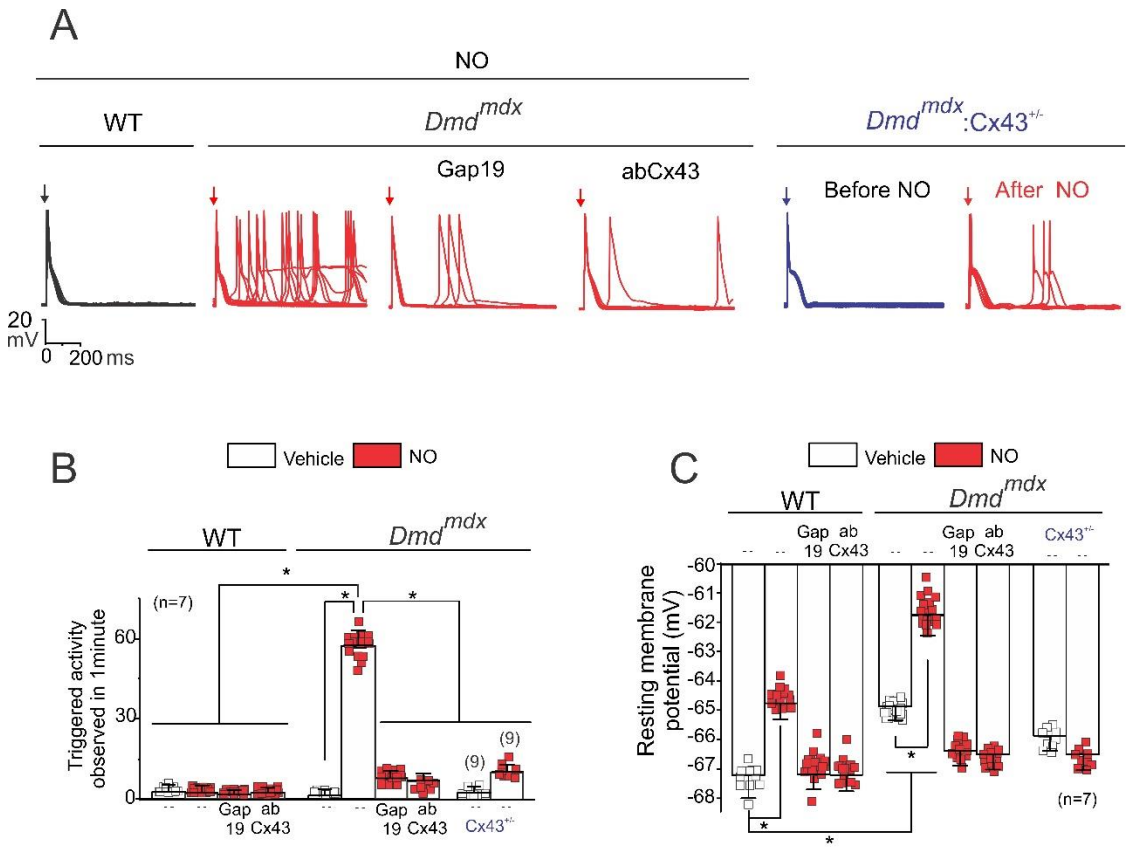

Fig 5. Exogenous nitric oxide-induced TA in *Dmd*^{mdx} cardiomyocytes.
A) Representative action potentials traces of WT, *Dmd*^{mdx} and *Dmd*^{mdx}Cx43$^{+/-}$ isolated cardiomyocytes. Cells were stimulated with 1 µM DEENO in the absence or presence of Cx43 hemichannel blockers, Gap19 (232ng/µL) and Cx43 CT antibody (abCx43; 2.5 ng/µL). Arrow indicates electrical stimulation pulse. **B)** Quantification of TA induced by DEENO in **(A).** The number in parentheses indicates the *n* value. Comparisons between groups were made using two-way ANOVA plus Tukey post-hoc test *P<0.05. **C)** Resting membrane potential of WT and *Dmd*^{mdx} cardiomyocytes upon DEENO stimulation. Comparisons between groups were made using two-way ANOVA plus Tukey post-hoc test, *P<0.05.

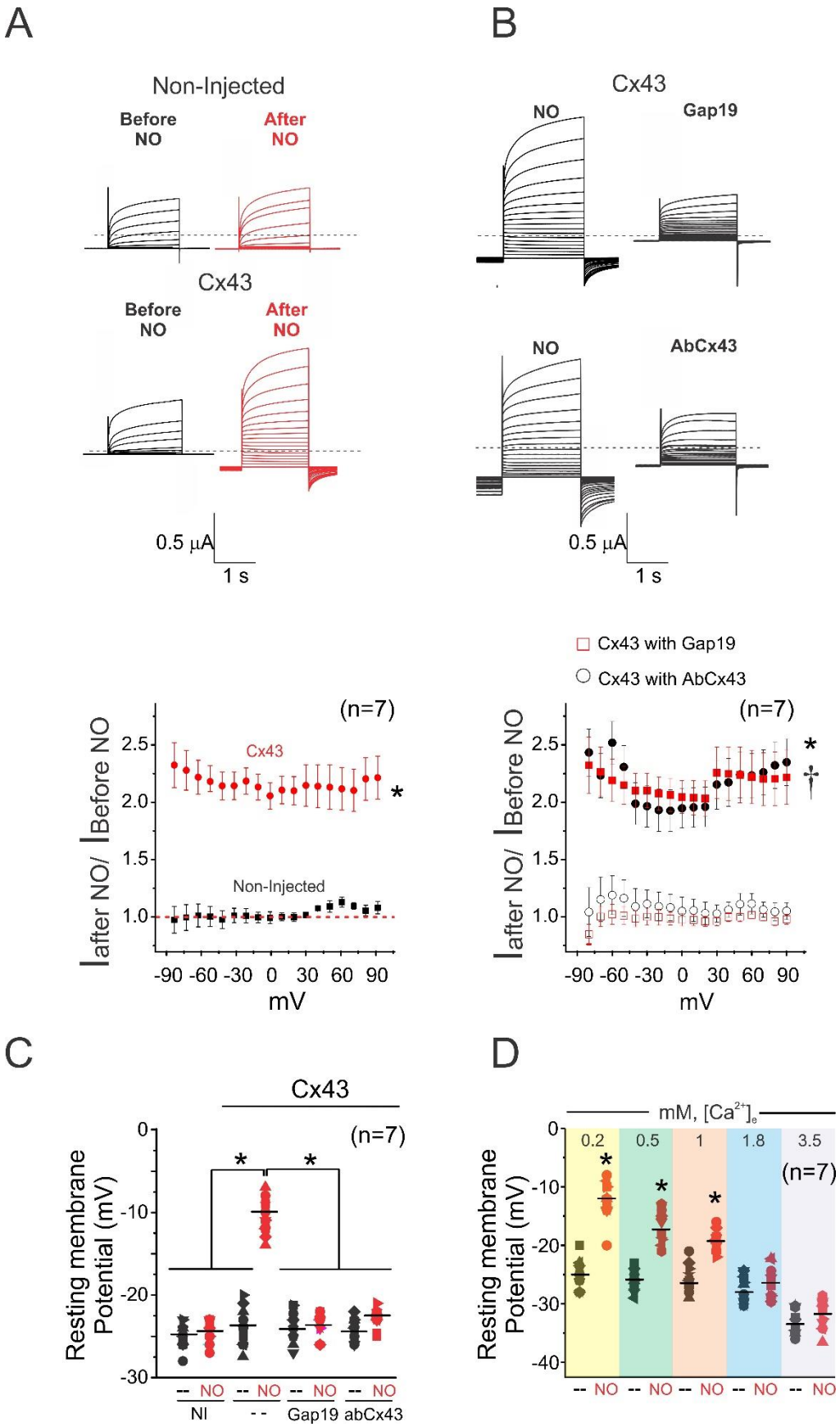
A
Non-Injected
Before NO
After NO
Cx43
Before NO
After NO
0.5 µA
1 s
B
Cx43
NO
Gap19
NO
AbCx43
0.5 µA
1 s
Cx43 with Gap19
Cx43 with AbCx43
(n=7)
Cx43
Non-Injected
I after NO/ I Before NO
mV
C
Cx43
(n=7)
Resting membrane Potential (mV)
-- NO -- NO -- NO -- NO
NI - - Gap19 abCx43
D
mM, [Ca2+]e
0.2
0.5
1
1.8
3.5
(n=7)
Resting membrane Potential (mV)
-- NO -- NO -- NO -- NO -- NO

990

Fig 6. Nitric oxide activated currents from oocytes expressing Cx43 hemichannels. **A)** Representative current traces before and after application of 10 μM DEENO in a non-injected oocyte or an oocyte expressing Cx43. Oocytes were clamped to −80 mV, and square pulses from −80 mV to +90 mV (in 10 mV steps) were then applied for 2s. At the end of each pulse, the membrane potential was returned to −80 mV. Normalized currents were obtained from the ratio between recorded current after and before DEENO treatment. The number in parentheses indicates the *n* value. Comparisons between groups were made using two-way ANOVA plus Tukey post-hoc test, *P<0.05 vs Non-Injected. **B)** Intracellular injection of Gap19 (232 ng/μL) or a Cx43 CT antibody (2.5 ng/μL) reduce NO-induced Cx43 hemichannels currents**.** The number in parentheses indicates the *n* value. Comparisons between groups were made using two-way ANOVA plus Tukey post-hoc test *P<0.05 vs Cx43 with Gap19; †<0.05 vs Cx43 with AbCx43. **C)** Changes in resting membrane potential in the presence or absence 10 μM DEENO. Cx43 hemichannel blockers restore normal resting membrane potential. Comparisons between groups were made using one-way ANOVA, *P<0.05. **D)** Extracellular calcium dependence of the resting membrane potential evoked by 10 μM DEENO in oocytes expressing Cx43 hemichannels. The number in parentheses indicates the *n* value. Comparisons between groups were made using two tailed Student's t test, *P<0.05 vs Control.

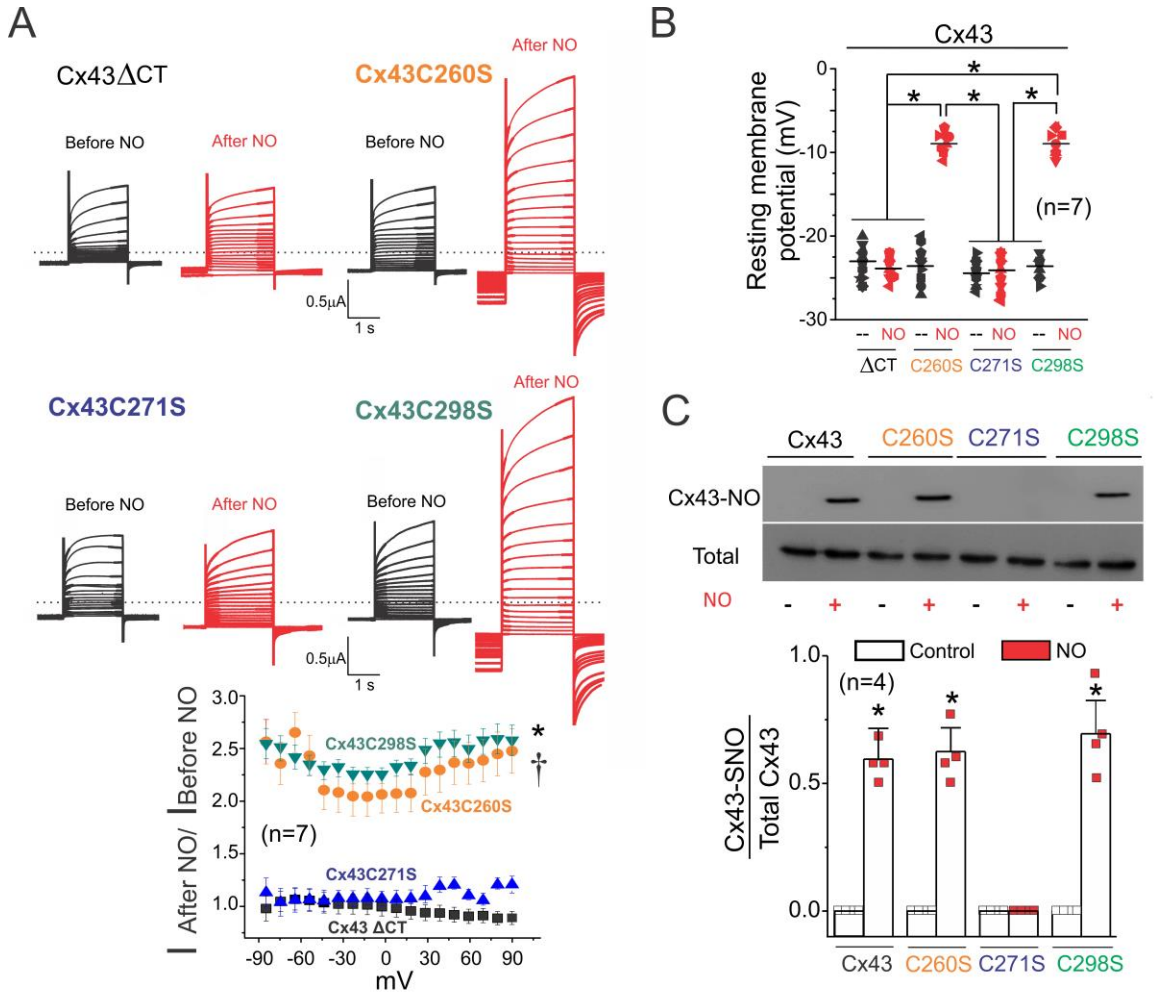

Fig 7. Position C271, but not C260 and C298, is S-nitrosylated and mediated NO-induce hemichannels currents.

A) Representative current traces for oocytes expressing Cx43 with a deleted carboxyl terminal (CT) and Cx43 mutants C260S, C271S and C298S. Black and red traces correspond to voltage step evoked currents in the absence or presence of 10 μM DEENO, respectively. Oocytes were clamped to −80 mV, and square pulses from −80 mV to +90 mV (in 10 mV steps) were then applied for 2s. At the end of each pulse, the membrane potential was returned to −80 mV. Graph shows normalized fold increased current DEENO after treatment at different voltages. The number in parentheses indicates the *n* value. Comparisons between groups were made using two-way ANOVA plus Tukey post-hoc test, *P<0.05 vs Cx43 ΔCT; †<0.05 vs Cx43C271. **B)** DEENO decreases the resting membrane potential in oocytes expressing Cx43 mutant C260S and C298S, but not in those expressing the Cx43 deleted CT or Cx43 mutant C271S. The number in parentheses indicates the *n* value. Comparisons between groups were made using two-way ANOVA test, *P<0.05 vs Control. **C)** Top gel is loaded with S-nitrosylated proteins pull down using the biotin switch assay and blot against Cx43. Bottom western blot were load with total proteins oocytes expressing Cx43 against Cx43. The number in parentheses indicates the *n* value. Comparisons between groups were made using Student's t test, *P<0.05 vs Control.